



# Organoboron chemistry comes to light: Recent advances in photoinduced synthetic approaches to organoboron compounds

Viet D. Nguyen, Vu T. Nguyen, Shengfei Jin, Hang T. Dang, Oleg V. Larionov\*

Department of Chemistry, The University of Texas at San Antonio, San Antonio, TX 78249, USA

## ARTICLE INFO

### Article history:

Received 31 October 2018

Received in revised form

11 December 2018

Accepted 19 December 2018

Available online 24 December 2018

### Keywords:

Borylation

Carboboration

Diboron reagents

Photochemistry

Organoboron compounds

Rearrangements

Ring contraction

## ABSTRACT

Photoinduced synthetic approaches to organoboron compounds have attracted significant attention in the recent years. Photochemical activation of organic molecules enables generation of reactive intermediates from a variety of precursors, resulting in borylation methods with improved and broader substrate scopes. The review summarizes recent developments in the area of photoinduced reactions of organoboron compounds with an emphasis on borylation of haloarenes, amine derivatives, and redox-active esters of carboxylic acids, as well as photoinduced rearrangements of organoboron compounds and photoinduced synthesis of organoboron compounds from alkenes and alkynes.

© 2018 Elsevier Ltd. All rights reserved.

## 1. Introduction

Organoboron compounds are among the most versatile classes of heteroatom-substituted organic molecules. Applications of boronic acids and their derivatives have seen a particularly dramatic surge in the past three decades (Fig. 1). In analytical chemistry, the mildly Lewis acidic character of the boron atom is exploited in the context of carbohydrate [1] and fluoride sensing [2] that is enabled by formation of tetracoordinate borates with fluoride anions and polyols. Boron is more electropositive than carbon, and this fundamental property is exploited to the fullest in organic synthesis that has become one of the most prominent areas of application of organoboron compounds. They serve as key nucleophilic coupling partners for a variety of C–C bond forming reactions, most notably the Suzuki–Miyaura reaction [3], as well as versatile synthetic intermediates derived from hydroboration [4] and carboboration reactions [5]. Boronic acids and their derivatives have also been successfully used as catalysts, e.g., for enantioselective reactions [6] and for the formation of amide bonds [7]. The recent explosive growth of materials science has led to new applications for boronic acids as building blocks for covalent organic

frameworks and hydrogels, as well as neutron capture and phosphorescent materials [8]. Another recent addition to boronic acids' repertoire is their emerging role as therapeutic agents and biological probes. In this arena, the first-in-class anticancer drug bortezomib has been joined by the recently approved antifungal tavaborole, and anti-eczema drug crisaborole, while many other boronic acid derivatives have shown promising activities in a large number of clinical and preclinical studies [9].

The most prevalent method of synthesis of boronic acids still relies on the reaction of borate esters with organomagnesium or organolithium reagents, as first described over 100 years ago by Khotinsky and Melamed [10]. In the meantime, new borylation methods have entered the synthetic scene. The most notable of them, the Pd-catalyzed borylation of aryl halides with diboron reagents developed by Miyaura [11] obviates the use of organometallic reagents that, in addition to air and moisture sensitivity, can suffer from low functional group tolerance. Miyaura borylation was further extended by Molander and Dreher to allow for a direct synthesis of boronic acids using tetrahydroxydiboron [12]. Other notable borylation approaches include transition metal-catalyzed C–H-borylation [13], transition metal-free, base-mediated borylation reactions of iodo- and bromoarenes [14], as well as electrophilic borylation of electron-rich arenes, alkynes and alkenes [15], Sandmeyer-type borylation of anilines [16], and catalytic

\* Corresponding author.

E-mail address: [oleg.larionov@utsa.edu](mailto:oleg.larionov@utsa.edu) (O.V. Larionov).

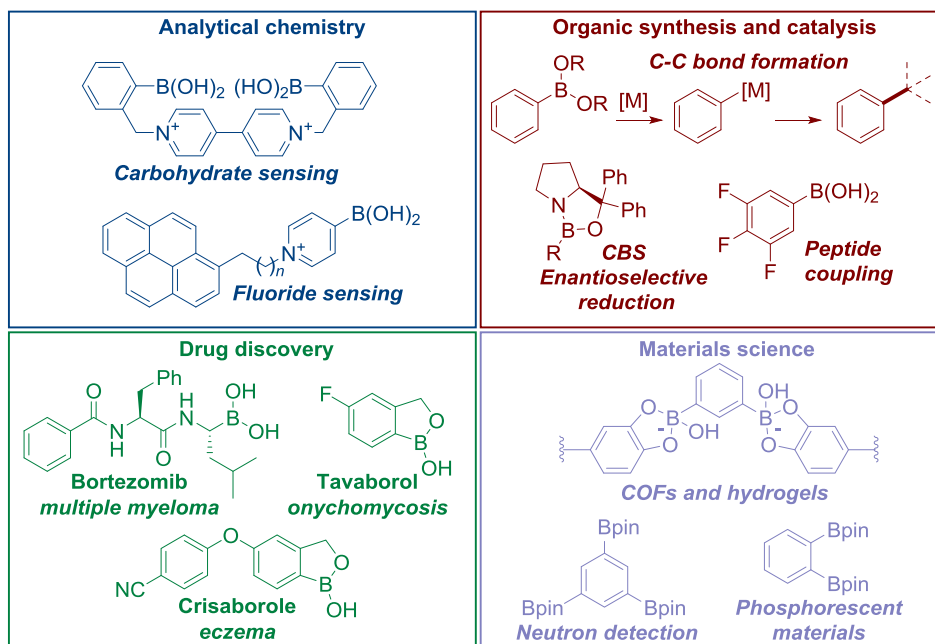


Fig. 1. Applications of organoboron compounds.

decarboxylative borylation of *N*-hydroxyphthalimide esters [17]. Photochemical activation allows for achieving new reactivity patterns and generation of highly reactive intermediates that would not be possible by thermal activation methods [18]. Photoactivation is particularly suitable for homolytic processes, although photoinduced heterolytic pathways are also available. Given the synthetic importance of aryl halides, a number of carbon–carbon and carbon–heteroatom bond-forming reactions, including nucleophilic substitution [19], arylation [20], alkylation [21], and photocyclization [22] have been reported that are based on the photoinduced Ar–X bond dissociation. The majority of photoinduced borylation reactions are enabled by radical intermediates that take part in homolytic substitution at one of the boron atoms of diboron reagents (Fig. 2). Homolytic substitution is a general type of reaction for organoboron compounds [23]. Although homolytic substitution at diboron reagents would produce boryl radicals that are inherently unstable and electron deficient species (as reflected in the high bond dissociation energies for B–H bonds) [24], the reaction could be made more thermodynamically favorable by prior formation of  $sp^2$ – $sp^3$  adducts of diboron reagents with Lewis bases. Such adducts have been observed and in some cases isolated (e.g., with fluoride, alkoxides, *N*-heterocyclic carbenes, 4-methylpyridine and phosphines) [25]. The Lewis base-stabilized boryl radicals that are produced from the  $sp^2$ – $sp^3$  adducts via homolytic substitution are substantially more stable, and they have previously been observed experimentally [26]. Consequently, most of the photoinduced borylation reactions have been rationalized in

terms of homolytic substitution at  $sp^2$ – $sp^3$  adducts of diboron reagents with Lewis bases that are present in the reaction, e.g., solvents, bases, and halide anions.

The various new photoinduced synthetic approaches that have appeared in the past decade will be classified by types of reactions. Synthesis of boronic acids and their derivatives by functional group interconversion of halides, carboxylic acids and amine derivatives comprises the largest category of the new methods, and it will be discussed first. Other approaches that make use of alkenes and alkynes will then be covered. Each class of transformations, when possible, will be discussed in the chronological order to highlight current trends in the development of photoinduced borylation and boration methods.

## 2. C–X borylation and related reactions

In 2016, Larionov and coworkers reported a photoinduced borylation of haloarenes, including electron-rich fluoroarenes, and quaternary arylammonium salts using tetrahydroxydiboron and other diboron reagents (Fig. 3) [27]. Diverse substituted arylboronic acids bearing functional groups including amide, hydroxy, and ester, as well as heteroarylboronic acids were prepared in good to excellent yields in methanol as a solvent. Aryl iodides and aryl chlorides were also transformed to the corresponding boronic acids, with the iodides giving the boronic acid products in excellent yields within 1 h, compared to 3–24 h in the case of aryl bromides and 24 h with lower yields for aryl chlorides. This reactivity pattern is in line with the increase in the bond dissociation energies (BDE) of Ar–X (C–I 272, C–Br 336, C–Cl 400 kJ mol<sup>−1</sup>) [28]. Interestingly, tavaborole (**1**), recently approved by the FDA for treatment of onychomycosis was readily prepared in good yield from the corresponding bromoarene following a straightforward workup. The reactions were performed in batch and flow, and also on gram scales.

Fluorobenzene that has a high BDE of the Ar–F bond (526 kJ mol<sup>−1</sup>) proved resistant to the borylation. However, fluoroarenes bearing electron-donating substituents are compatible with this transformation. (4-Aminophenyl)boronic acid and (4-

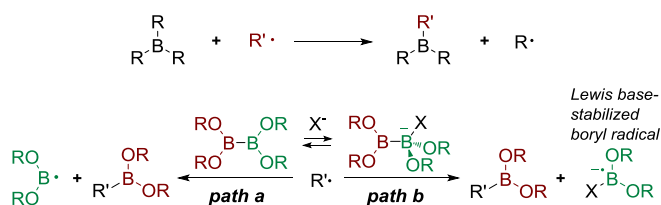


Fig. 2. Homolytic substitution at boron.

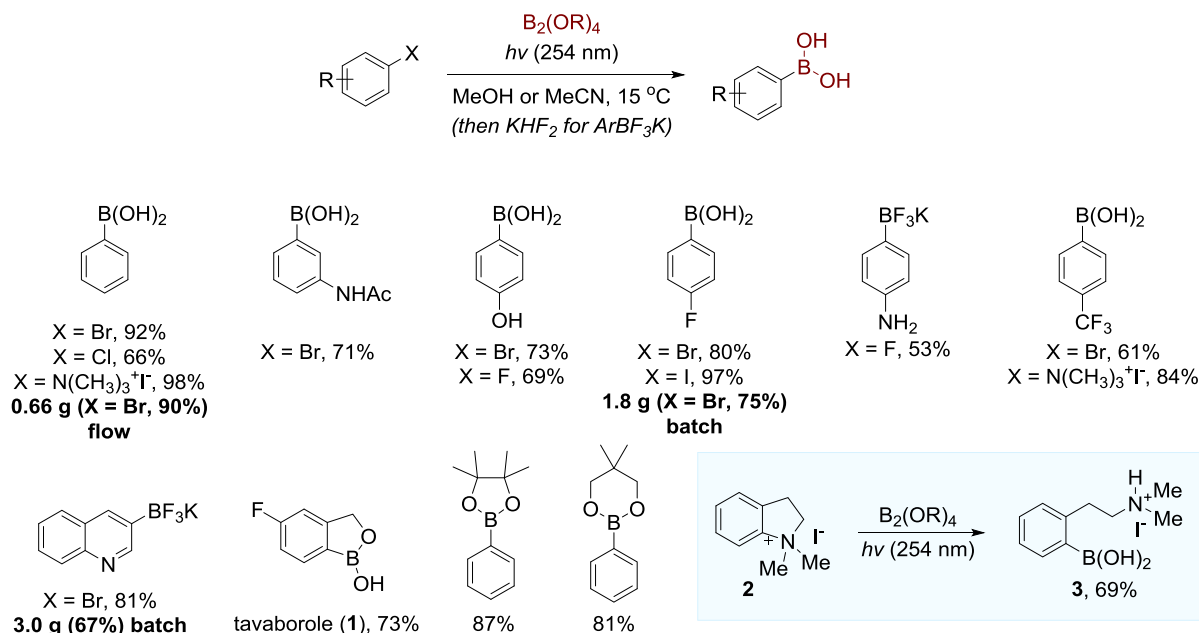


Fig. 3. Photoinduced borylation of haloarenes.

hydroxyphenyl)boronic acid were isolated as trifluoroborates in good yields from corresponding unprotected fluoroarenes. For the photoinduced borylation of fluoroarenes, it was suggested that the generation of the triplet aryl cation via the heterolysis of the C–F bond first takes place, which is then followed by the formation of a transient  $sp^2$ - $sp^3$   $\text{B}_2(\text{OR})_4\text{F}^-$  species and the subsequent reaction between those two species. The borylation of Ar–N bond was also investigated for arylammonium iodides. Various boronic acids were prepared from corresponding arylammonium iodides in good to excellent yields. Thus, cyclic salt **2** gave boronic acid **3** in good yield.

Besides tetrahydroxydiboron, various diboron esters were employed as effective borylation reagents, producing corresponding phenylboronic esters in acetonitrile as a solvent. A detailed experimental procedure was subsequently reported to facilitate the use of the photoinduced borylation method [29].

Mechanistically, initial excitation is followed by intersystem crossing to triplet **4** (Fig. 4). Three divergent pathways were proposed for the subsequent borylation. In the first pathway, homolysis of triplet **4** leads to generation of aryl radical **5** that produces boronic acid or ester **6** and radical intermediates **7** or **8** upon homolytic substitution in diboron species **9** or **10**. Alternatively, the homolytic substitution can produce anion radical **11**. In the second pathway, heterolysis of triplet **4** produces triplet aryl cation **12** that further reacts with in diboron species **9** or **13** to give cation radical **14** and anion radicals **15** or **16**. Subsequent single electron transfer (SET) produces boronic acid or ester **6**. Given the relatively high photochemical quantum yield ( $\Phi = 0.34$ ), a radical chain pathway was also proposed that involves single electron transfer from anion radical species **7** or **11** to triplet **4** or the ground state haloarene, resulting in aryl radical **5** via the intermediacy of anion radical **17**.

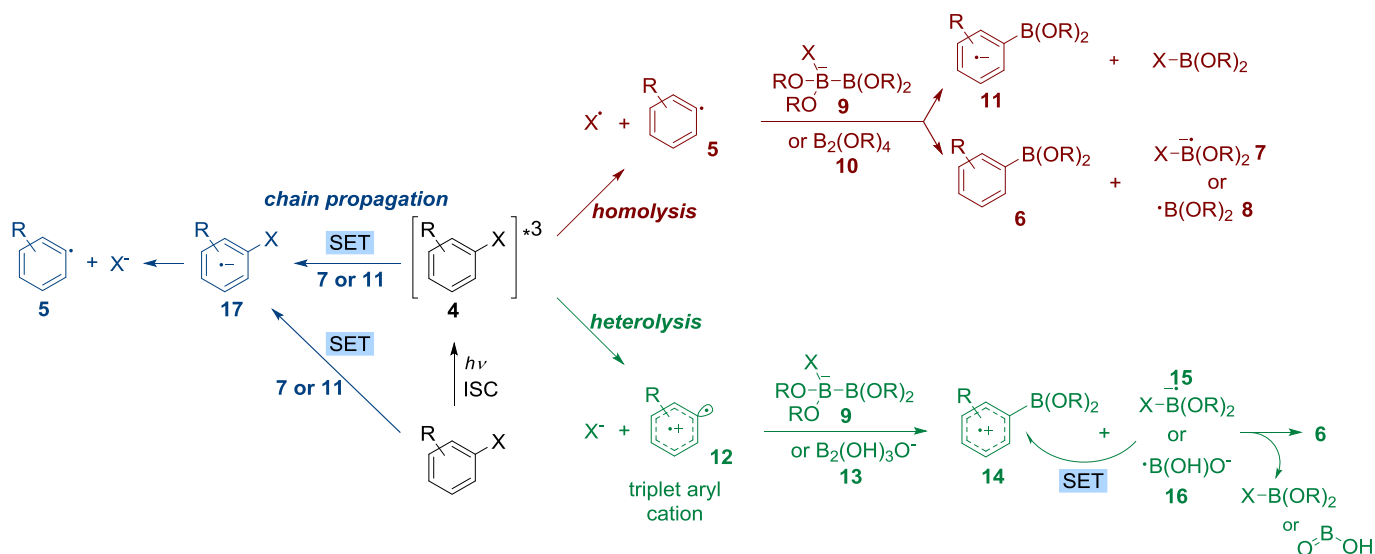


Fig. 4. Mechanism of photoinduced borylation of haloarenes.

Following up on the photoinduced monoborylation of haloarenes, Larionov and coworkers further reported an additive- and metal-free photoinduced regioselective 1,2- and 1,3-C–H/C–X diborylation of haloarenes in the same year [30]. A notable feature of this method is the strong influence of the solvent on the regioselectivity of the diborylation. While monoborylation is observed in low viscosity solvents (methanol and acetonitrile), a higher viscosity solvent (isopropanol) leads to formation of 1,2-diborylation product **18** and 1,3-diborylation product **19** in 5.3:1 ratio from bromobenzene (Fig. 5). This result was explained by the reaction between monoborylation product **20** and the Bpin radical that are formed in the homolytic substitution step. Confinement of intermediate **20** and the Bpin radical in the solvent cage of isopropanol enables addition of the Bpin radical to boronic ester **20** that leads to radical **21**. The ortho-selectivity was explained by the stabilization of the radical through conjugation with the boryl group.

On the other hand, in the very polar hexafluoroisopropanol (HFIP) 1,3-C–H/C–X diborylation was observed with a high regioselectivity (**19/18/22** ratio 42:5:1) (Fig. 6). In this case, it was proposed that the photoinduced heterolytic cleavage generates triplet aryl cation **12** that further undergoes borylation with the  $sp^2$ - $sp^3$  diboron adduct **23**. The resulting cation radical **14** and anion radical **24** further react to give the cationic intermediate **25** that is less destabilized by the electron-withdrawing boryl substituent than cation **26**, resulting in meta-product **19**. However, the 1,3-substitution pattern induced by weak  $\pi$ -acceptor boryl group can change to 1,2-diborylation if a stronger electron-withdrawing or electron-donating group is present in the para or meta position of the haloarene (Fig. 7). High yields were observed for 2- and 4-alkyl-, as well as 2,3-dialkyl- substituted haloarenes in HFIP. In addition, fluoro and chloro groups were tolerated, and the sterically hindered mesitylene also afforded 1,3-diborylation product in good yield. Iodoarenes bearing electron-acceptor groups, e.g., pentafluorosulfanyl, trifluoromethyl, boryl and cyano groups gave the expected single regioisomers of 1,2- or 1,3-diborylation products with the regioselectivity determined by the substituents (Fig. 7).

The reaction was successfully used to prepare diborylation products on gram scales under batch and continuous flow conditions. HFIP was efficiently recovered by distillation and reused for subsequent diborylation reactions. In addition, UV-transparent plastic vessels were used for batch applications instead of quartz glassware.

In 2016, Li and coworkers reported a photoinduced borylation of haloarenes in the presence of TMDAM ( $N,N,N',N'$ -tetramethyldiaminomethane) (**27**) in aqueous methanol for boronic acids or a

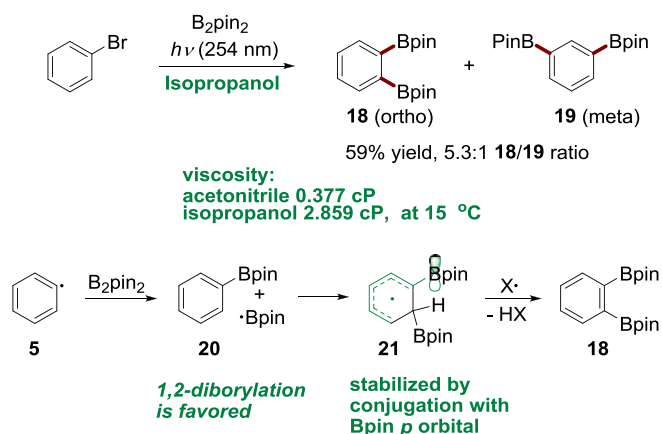


Fig. 5. 1,2-C–H/C–X diborylation of haloarenes in isopropanol.

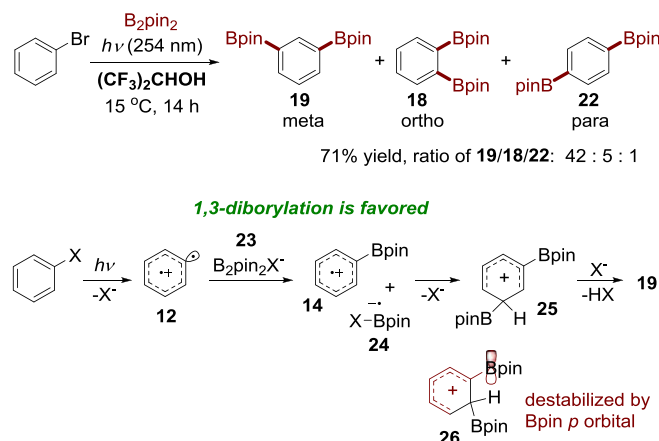


Fig. 6. 1,3-C–H/C–X Diborylation of haloarenes in hexafluoroisopropanol.

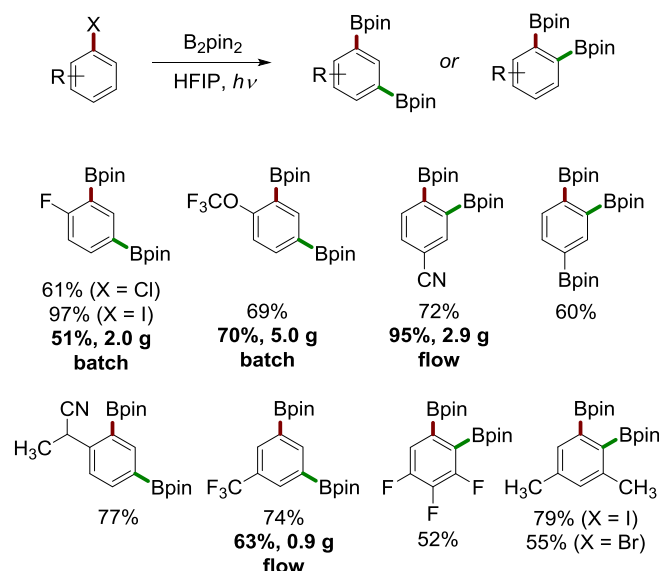


Fig. 7. Products of 1,2- and 1,3-C–H/C–X diborylation of haloarenes in hexafluoroisopropanol.

mixture of acetonitrile, acetone and water for boronic esters (Fig. 8) [31]. Interestingly, performing the reaction in a continuous-flow setup not only improved the reaction yield but also reduced the amount of  $B_2pin_2$  (1.5 equiv. compared to 2 equiv. in a batch setup) and the reaction time (15 min compared to 4 h in a batch setup). A variety of electron-donating, and electron-withdrawing substituents including hydroxy, amino and carbonyl groups were well-tolerated, giving corresponding boronic acids and esters in good to excellent yields. Aryl iodides afforded borylation products in higher yields than aryl bromides.

Mechanistically, the borylation is thought to be initiated by the photoinduced homolytic cleavage of the Ar–X bond (Fig. 9). Aryl radical intermediate **5** further reacts with  $sp^2$ - $sp^3$  diboron adduct **28** formed in the reaction between TMDAM (**27**) with  $B_2pin_2$  in the presence of water, affording borylation product **6**. Given the importance of TMDAM (**27**) for the reaction (e.g., a low yielding borylation is observed with TMDAM in the dark), single electron transfer pathway from both ground state and excited haloarene to give anion radical **17** and cation radical **29** was also proposed. Finally, boron-containing anion radical **30** that is initially produced

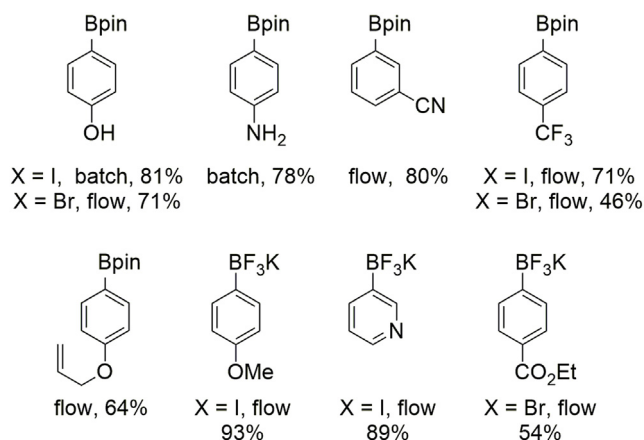


Fig. 8. Photoinduced borylation of aryl bromides and iodides in the presence of TMDAM (27).

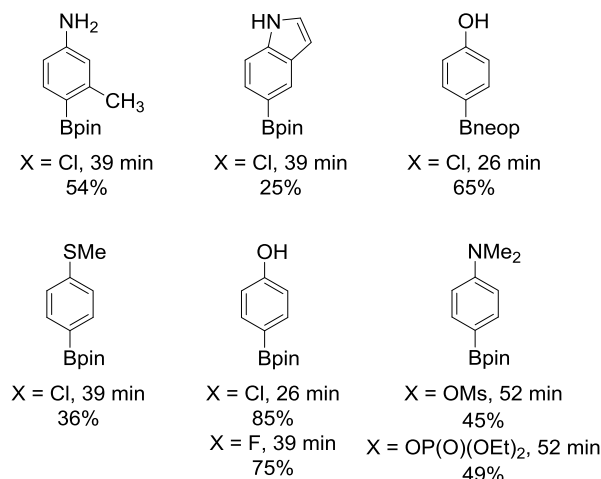
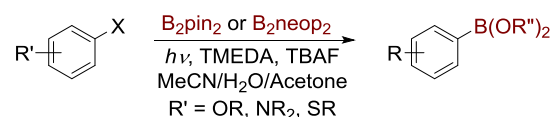


Fig. 10. Photoinduced borylation of electron-rich aryl chlorides, fluorides, and pseudohalides.

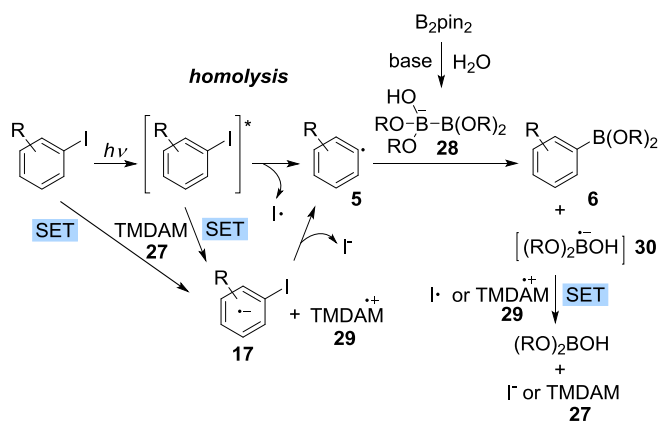


Fig. 9. Mechanism of photoinduced borylation of aryl bromides and iodides in the presence of TMDAM (27).

in the homolytic substitution step is quenched by SET with iodide radical or cation radical **29**.

In the same year, Li and coworkers further expanded the scope of their photoinduced borylation method to electron-rich aryl chlorides, fluorides, mesylates and phosphates (Fig. 10) [32]. The reaction was carried out in a continuous flow reactor with 1.5–2 equiv. of  $\text{B}_2\text{pin}_2$ , 0.5 equiv. of TMEDA ( $N,N,N',N'$ -tetramethylethylenediamine) and 0.1 equiv. of TBAF in a mixture of acetonitrile, acetone and water.

The reaction mixture was irradiated by a 300 W high pressure mercury lamp with the retention time ranging from 26 min to 1 h. Chloroarenes containing strong electron-donating substituents including O-, S-, and N-derived groups in the *ortho*- or *para*-position afforded corresponding boronic esters. Several aryl fluorides, mesylates and phosphates were also successfully converted to corresponding boronic esters. Aryl triflates, on the other hand, were found to be ineffective, due to hydrolysis. Electron-neutral and electron-deficient aryl chlorides were unreactive under the reaction conditions. Based on experimental and computational data,

the mechanism is thought to involve formation of a triplet aryl cation, whose energy is  $1.4 \text{ kcal mol}^{-1}$  lower than that of the singlet species, via photoinduced heterolytic cleavage of  $\text{Ar-X}$  bond. Subsequent three-component combination of the triplet aryl cation, chloride anion and  $\text{B}_2\text{pin}_2$  passes through a singlet transition state via a crossing point between the triplet and singlet potential energy surfaces, resulting in the ground state borylation product.

The photoinduced borylation was recently successfully used by Sarpong and coworkers in the context of total synthesis of monomeric and dimeric stephacidin A (**31**) congeners from ketopremalbranchamide (**32**) (Fig. 11) [33]. It was found that ketopremalbranchamide (**32**) can be readily converted to malbranchamide C (**33**) via a remarkable sequence of C3 bromination and C3 to C6 bromine translocation that is followed by regioselective amide reduction. However, the analogous C6 chlorination approach en route to malbranchamide B (**34**) could not be accomplished. Thus, malbranchamide C (**33**) was subjected to photoinduced borylation to give boronic ester **35** that was successfully chlorinated with copper dichloride.

In addition, the preparation of (+)-stephacidin A (**31**) called for installation of a hydroxyl group at C6 in ketopremalbranchamide (**32**). The C6 hydroxylation was likewise accomplished by photoinduced borylation of iodoindole **36**, followed by oxidation to give hydroxyindole **37** in a 55% yield over two steps. The authors mentioned that the photoinduced borylation reactions developed by P. Li and Larionov were the only borylation methods that produced the desired products among several protocols that were tested.

In 2016, Fu and coworkers reported a visible light-induced photoredox-catalyzed borylation of haloarenes using iridium photocatalyst **38** (Fig. 12). The authors also showed that the borylation can be combined with subsequent aerobic oxidation of the boronate products to phenols [34]. In the model reaction of *p*-iodoanisole with bis(pinacolato)diboron, iridium photocatalyst **38** (*fac*- $\text{Ir}(\text{ppy})_3$ ) demonstrated optimal performance with tributylamine as a sacrificial reduction agent. Aqueous acetonitrile proved to be the



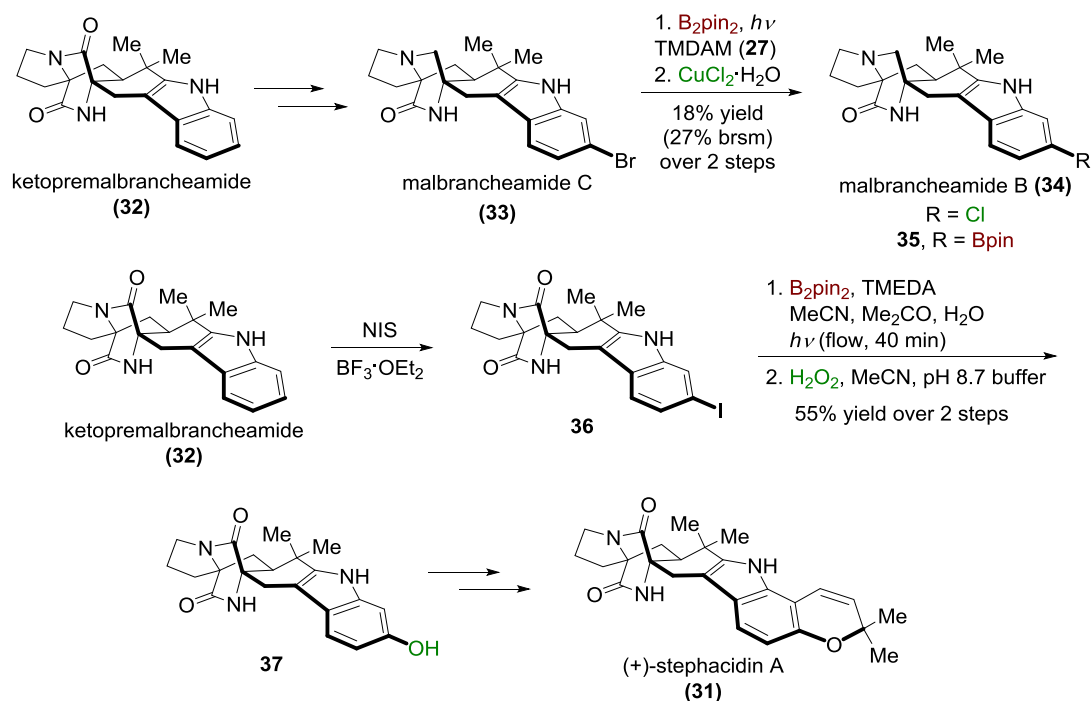


Fig. 11. Application of photoinduced borylation in Sarpong's synthesis of (+)-stephacidin A (31).

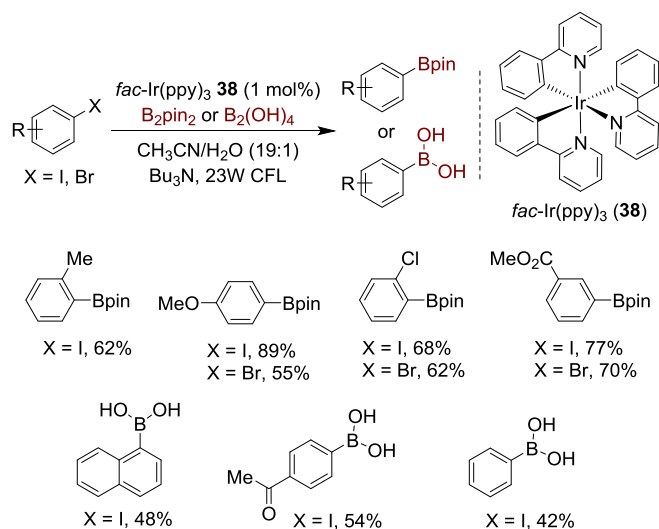


Fig. 12. Visible light-induced photoredox borylation of aryl bromides and iodides.

solvent of choice for this reaction. Replacement of tributylamine with other amines (e.g., triethylamine or diisopropylethylamine) resulted in lower yields. The generality of the method was examined with a number of bromo- and iodoarenes (Fig. 12). A variety of functional groups were tolerated the reaction including ether, ketone, nitrile, ester and aldehyde groups. In general, iodoarenes were more reactive than bromoarenes. Aryl iodides bearing both electron-donating and electron-withdrawing substituents performed equally well. On the other hand, electron-deficient aryl bromides gave higher yields of borylation products than electron-rich aryl bromides. Boronic acids were also prepared using this method with tetrahydroxydiboron, however, only aryl iodides were

found to be suitable substrates, and the yields were lower than for boronic esters. The reaction was also tested with alkyl bromides under standard conditions, – moderate yields were obtained. Finally, one-pot, two-step reaction including borylation of aryl halides and hydroxylation of arylboronic esters to afford phenols was conducted. Moderate to good yields were observed for the isolated phenols, proving that aryl halides can be converted to phenols by using the developed borylation/oxidation protocol.

Involvement of hydroxide-diboron adduct **39** is postulated to be promoted by the amine in the aqueous acetonitrile solution (Fig. 13). A SET oxidation of the amine by the photoexcited iridium catalyst generates  $Ir^{II}$  species that transfers an electron to aryl halide. The transient anion radical **40** produces aryl radical that

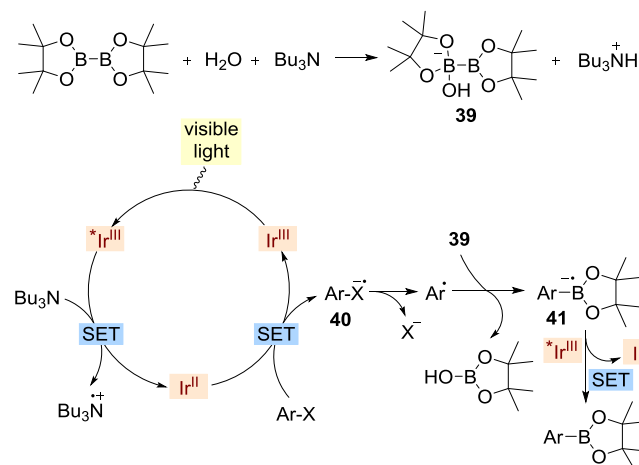


Fig. 13. Mechanism of visible light-induced photoredox borylation of aryl bromides and iodides.

further reacts with diboron adduct **39** to give anion radical intermediate **41**, which can serve as reductive quencher for the photoexcited Ir catalyst. Brief experimental and EPR studies were performed, and the experimental evidence supported the proposed mechanism. However, it should be pointed out that catalyst **38** ( $E_{1/2}(\text{Ir}^{\text{III}*}/\text{Ir}^{\text{II}}) = +0.31$  V vs SCE in MeCN) [35] may not be able to oxidize the tertiary amine ( $E_{1/2}^{\text{red}} = +0.99$  V vs SCE in MeCN for triethylamine) [36], but it may be a sufficiently strong reductant ( $E_{1/2}(\text{Ir}^{\text{IV}}/\text{Ir}^{\text{III}*}) = -1.73$  V vs SCE in MeCN) [35] to mediate the SET-induced cleavage of the aryl halides, as previously shown by Stephenson and coworkers [37].

Generation of aryl radicals from aryl triflates is challenging, due to the ease of the S–O bond cleavage that outcompetes the C–O bond cleavage [38] and the propensity to undergo hydrolysis, as discussed above for P. Li's photoinduced borylation method. Based on their earlier work [39], C.-J. Li and coworkers developed a metal-free method of generation of aryl radicals from aryl triflates and applied it to synthesis of aryl boronates (Fig. 14) [40]. Specifically, the authors observed that photoinduced borylation of aryl triflates takes place in the presence of TMDAM and NaI. The system is close to the one reported earlier by P. Li [32], but it produces aryl boronates in higher yields. Various substituted boronic esters could be obtained with this protocol. The authors proposed that the aryl triflate radical anion is first produced by a photoinduced SET from the iodide anion, due to its noticeable reducing ability (path a, Fig. 15). The aryl triflate radical anion further produces aryl radical **5** and the triflate anion. Aryl radical **5** can then engage  $\text{B}_2(\text{Pin})_2$  in homolytic substitution at boron. This mechanism does not account for the role of TMDAM (**27**), and, since aryl iodides can also be obtained from aryl triflates, involvement of transient aryl iodides that undergo TMDAM-induced SET reduction (path b, Fig. 15) as proposed by P. Li [32] cannot be ruled out.

Cerium complexes have recently attracted attention as photocatalysts, due to the relative abundance of cerium and their favorable photophysical properties [41]. Continuing their work on the photocatalysis with cerium complexes [41b–d], Schelter and coworkers developed a photoinduced borylation of aryl halides catalyzed by hexachloroate ( $[\text{Ce}^{\text{III}}\text{Cl}_6]^{3-}$ ) anion (Fig. 16) [42]. The team, in collaboration with Anna and coworkers, had previously

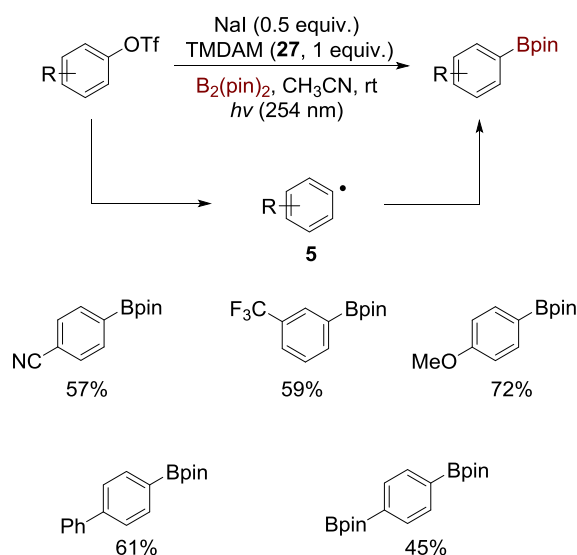


Fig. 14. Synthesis of aryl boronates from aryl triflates as radical precursors.

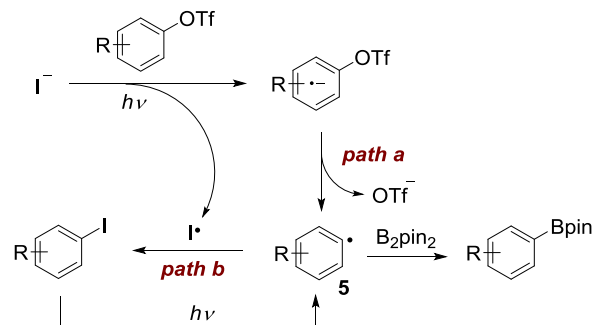


Fig. 15. Mechanism of photoinduced borylation of aryl triflates in the presence of iodide.

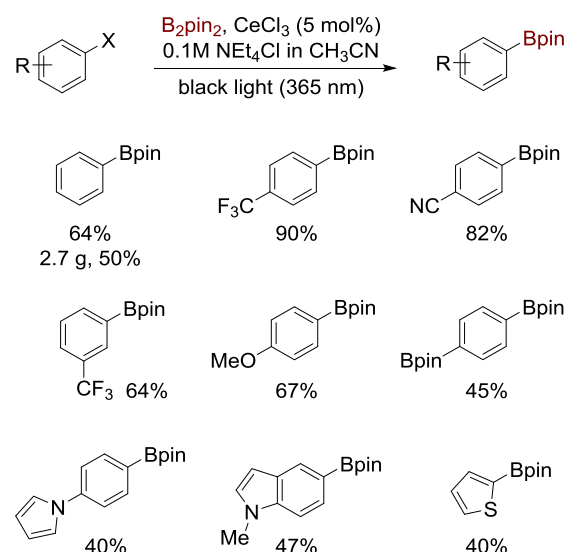


Fig. 16. Photoinduced, hexachloroate(III)-catalyzed borylation of aryl chlorides and bromides.

discovered that  $[\text{Ce}^{\text{III}}\text{Cl}_6]^{3-}$ , which can be generated in situ from  $\text{CeCl}_3$  and  $\text{NEt}_4\text{Cl}$  in acetonitrile is a potent photoreductant, which can mediate single electron transfer reductions of aryl bromides and chlorides [41d]. Combining hexachloroate(III) photocatalysis with radical borylation mediated by diboron reagents, they obtained a variety of aromatic boronic esters (Fig. 16).

Chloroarenes and bromoarenes bearing electron-donating and electron-withdrawing groups in the *para*, *meta*, and *ortho* positions, were converted into the corresponding borylation products, although lower yields were observed for *ortho*-substituted and heteroaryl products, in the latter case possibly due to coordination of the substrates to the cerium cation. The high quantum yield ( $\Phi = 6.1$ ) points to a radical chain process. The reaction is thought to be initiated by a single electron transfer from the photoexcited hexachloroate(III) anion to haloarene (Fig. 17). The resulting aryl radical further reacts with diboron reagent and chloride anion to give the borylation product and radical anion **42**. Radical anion **42** can further propagate the chain by reacting with haloarene to give radical anion **43** and product **41**. A reaction of radical anion **43** with  $\text{B}_2\text{pin}_2$  regenerates radical anion **42**. The photogenerated hexachloroate(IV) is reduced via photoinduced ligand to metal charge transfer (LMCT) that produces radical anion **43** upon ligand exchange with chloride anion from  $\text{Et}_4\text{NCl}$ . Reaction of radical

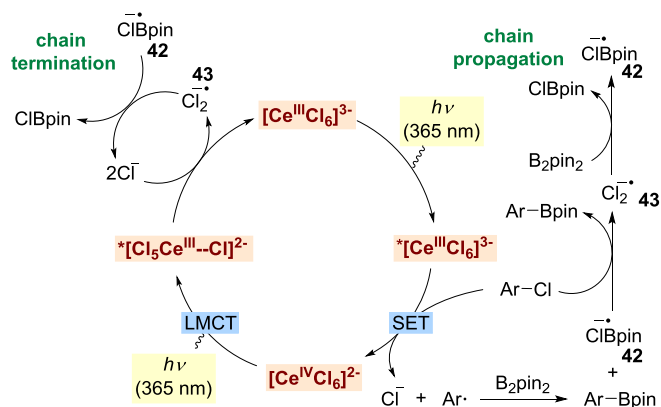


Fig. 17. Mechanism of photoinduced, hexachloro-cerate(III)-catalyzed borylation of aryl chlorides and bromides.

anions **42** and **43** is thought to terminate the radical chain process.

Following up on their earlier-reported metal-free 1,2-carboboration reaction (see Section 5) [43], Studer and coworkers developed a blue LED light-induced borylation of alkyl and aryl iodides with bis(catecholato)diboron,  $\text{B}_2\text{cat}_2$ , (**44**) in DMF (*N,N*-dimethylformamide) as a solvent (Fig. 18) [44]. The intermediate catecholato-boronic esters were converted to Bpin esters in a reaction with pinacol and trimethylamine to facilitate isolation.

The reaction has a broad scope with respect to alkyl iodides. Thus, primary, secondary and tertiary alkyl iodides were efficiently converted to the corresponding boronic esters in good to excellent yields. Aryl iodides also proved to be suitable substrates, including the *ortho*-substituted 2-iodotoluene. 1-Cyclohexenyl iodide also produced the corresponding boronic ester, albeit in a lower yield. Radical clock kinetic measurements were carried out to determine the rate constants for the reaction of the intermediate radical with  $\text{B}_2\text{cat}_2$ . Interestingly, the results of the study suggest that primary alkyl radicals react at a rate that is comparable to that of the reduction with  $\text{Bu}_3\text{SnH}$ . Aryl radicals, on the other hand, react one order of magnitude slower, likely due to the rate-dampening steric interactions.

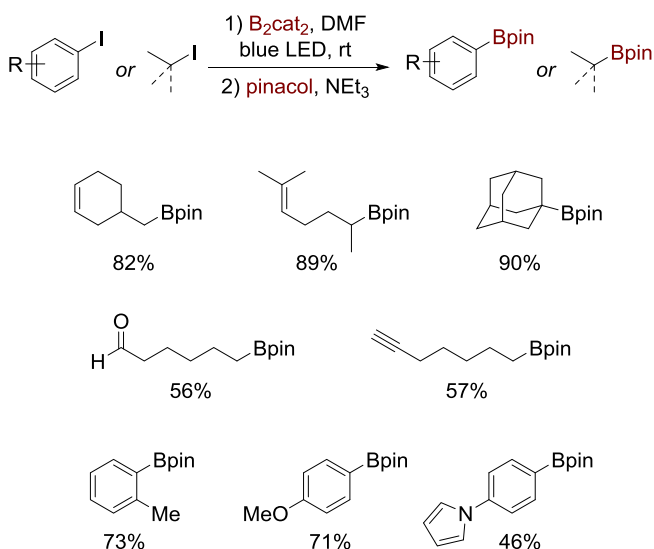


Fig. 18. Blue LED light-induced borylation of alkyl and aryl iodides.

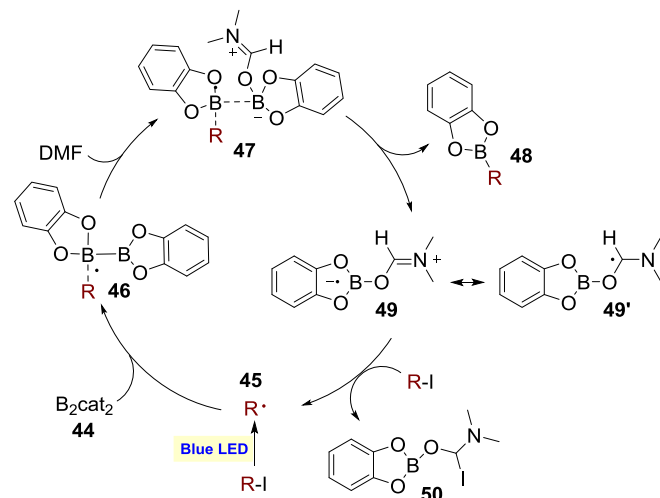


Fig. 19. Mechanism of the borylation of alkyl and aryl iodides with  $\text{B}_2\text{cat}_2$  (**44**) in DMF.

A detailed computational study was also performed that expanded on the previously suggested mechanism for the blue LED-induced 1,2-carboboration. The borylation is thought to be initiated by photoinduced homolysis of the C-I bond (Fig. 19). The produced radical **45** reacts with  $\text{B}_2\text{cat}_2$  (**44**) to give intermediate **46** that cannot undergo direct homolytic cleavage of the B-B bond, due to the high thermodynamic and kinetic costs of the process. Instead, an intermediate **47** is formed in a reaction with a molecule of DMF. The homolytic splitting of intermediate **47** into borylation product **48** and a radical intermediate represented by resonance structures **49** and **49'** is thermodynamically and kinetically favored. Computational studies indicate that the spin density in **49/49'** is much higher at the C atom in the O-C-N fragment than at the boron atom. Thus, subsequent reaction of intermediate **49/49'** produces iodide **50**, regenerating radical **45** via a kinetically-favored iodine atom abstraction.

The area of photoinduced Ar-X borylation has experienced a rapid growth in the past two years. While the catalyst-free methods are operationally simple and readily scalable, photoredox-catalyzed approaches can offer complementary substrate scopes and the practicality of the visible light-induced methodology. While only two of the methods have so far been evaluated in the context of complex target-oriented synthesis, the area will continue to expand, and new practical photoinduced Ar-X borylation methods will no doubt enter the synthetic scene in the near future.

### 3. Decarboxylative borylation

Glorius and coworkers devised a decarboxylation-based method for conversion of *N*-hydroxyphthalimide (NHPI) esters of abundant aromatic carboxylic acids **51** to aromatic boronic esters (Fig. 20) [45]. The decarboxylative borylation reaction of NHPI esters **51** tolerated a broad range of substrates. Carboxylic acids bearing electron-donating or electron-withdrawing substituents in *para*- or *meta*-positions performed well in the reaction and afforded aryl boronic esters in good yields. However, the more electron deficient tetrachlorinated *N*-hydroxyphthalimide was required for the borylation of electron-deficient carboxylic acids. Borylation of *ortho*-substituted acids was challenging, and the products were isolated in low yields. Acids containing naphthalenes or heteroaromatic cores, e.g., quinoline, indole, pyridine, and thiophene were successfully borylated in moderate to good yields. Cinnamic acid was



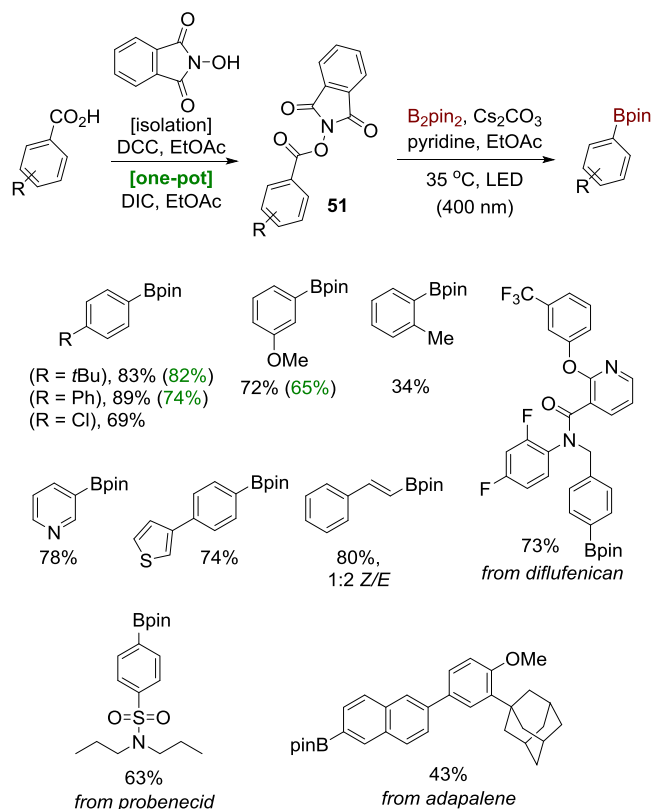


Fig. 20. Visible light-induced borylation of NHPI esters of aromatic carboxylic acids.

converted to a vinyl boronic ester in 80% yield but with 1:2 Z/E ratio. The reaction performed well with aryl halides, affording borylated aryl halides that can undergo two sequential coupling reactions to form difunctionalized arenes. Furthermore, the decarboxylative borylation was utilized to modify two active pharmaceutical ingredients, – probenecid and adapalene, as well as a derivative of herbicide diflufenican.

Functional group tolerance was additionally investigated by a robustness screen [46] that showed that reaction performed well with alkynes, ketones, aldehydes, alcohols, but it was shut down by anilines and furans. Additionally, the transformation can be carried out with carboxylic acids as starting materials in one-pot procedure without purification of NHPI esters.

Mechanistically, it is proposed that the reaction is initiated by photoexcitation of *N*-hydroxyphthalimide ester **51** (Fig. 21). The excitation is followed by intersystem crossing to generate triplet excited intermediate **52**.  $B_2pin_2$  forms  $sp^2$ - $sp^3$  diboron complex **53**

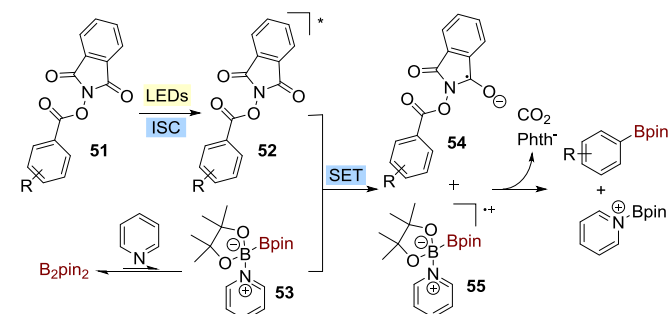


Fig. 21. Plausible mechanism of visible light-induced borylation of NHPI esters **51**.

with pyridine, as previously described by Jiao [14i]. A single electron transfer then takes place between triplet intermediate **52** and diboron complex **53** yielding radical anion **54** and radical cation **55**. This conclusion results from the analysis of fluorescence quenching of photoexcited ester **51** by the combination of  $B_2pin_2$  and pyridine. The radical anion **54** subsequently fragments into  $CO_2$ , phthalimide anion and an aryl radical that undergoes borylation by boron transfer from anion radical **55**. Indeed, formation of HO-Bpin that was confirmed by  $^{11}B$  NMR spectroscopy and the failure of radical traps to intercept the transient aryl radical suggest that the insolvent-cage borylation takes place after the rapid decarboxylation process.

In 2017, Li and coworkers described a photoredox-catalyzed borylation of *N*-hydroxyphthalimide esters of readily available aliphatic acids **56** (Fig. 22) [47].

The decarboxylative borylation proceeded well in DMF with iridium complex **57** as a photoredox catalyst, producing boronic acids that were converted to easily-isolated potassium alkyltri-fluoroborates with aqueous  $KHF_2$  in moderate to good yields. On the other hand, the use of a ternary solvent mixture facilitated the conversion of primary alkyl carboxylic acids into boronic esters derivatives. Primary and secondary carboxylic esters were found to be suitable substrates, tertiary carboxylic esters, on the other hand, only led to alkanes, likely due to competing decarboxylation and hydrogen atom abstraction.

Carboxylic acid bearing esters, ketones, carbamates, ethers, alkenes, terminal alkynes, and halides performed well. Four to six-membered carbocyclic and heterocyclic borylation products were readily prepared using this method. However, the borylation of NHPI esters of aromatic acids **51** was inefficient, e.g., only 10% yield of *m*-toluic acid. It is proposed that upon irradiation the photoexcited Ir catalyst reduces NHPI ester **56**, generating anion radical **58** and the oxidizing  $Ir^{IV}$  species (Fig. 23). Homolytic cleavage that is followed by decarboxylation of intermediate **58** affords  $CO_2$ , phthalimide anion, and alkyl radical **45**.

Nucleophilic  $sp^2$ - $sp^3$  diboron adduct **9** can be generated by a

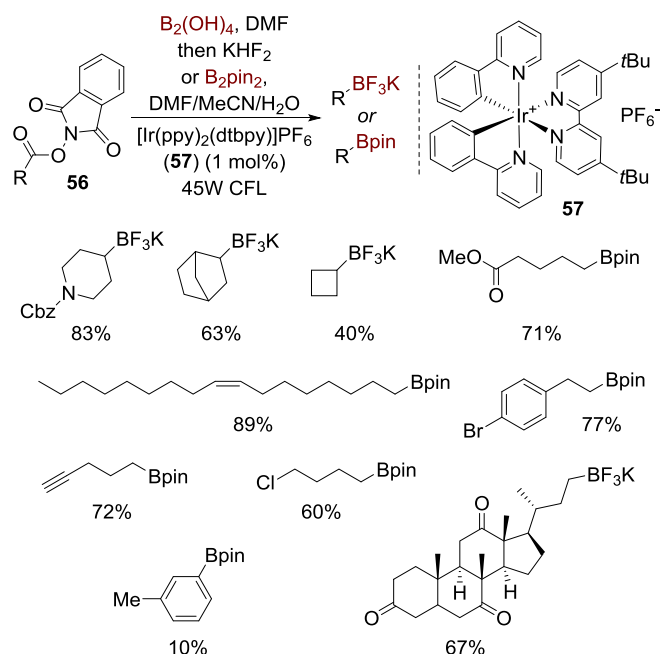


Fig. 22. Borylation of aliphatic NHPI esters **56**.

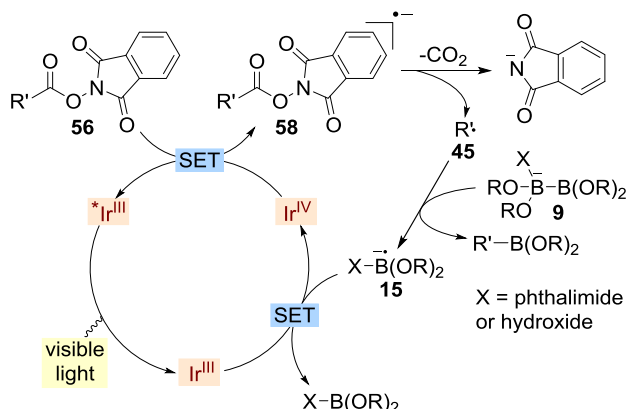


Fig. 23. Mechanism of photoredox-catalyzed borylation of NHPI esters **56**.

reaction of diboron reagent  $B_2(OR)_4$  with phthalimide anion or hydroxide anion – the product of protonation of phthalimide anion in the presence of water. Diboron reagent **9** then reacts with alkyl radical **45**. Radical anion **15** that is produced in this reaction reduces  $Ir^{IV}$  species, regenerating the photoredox catalyst.

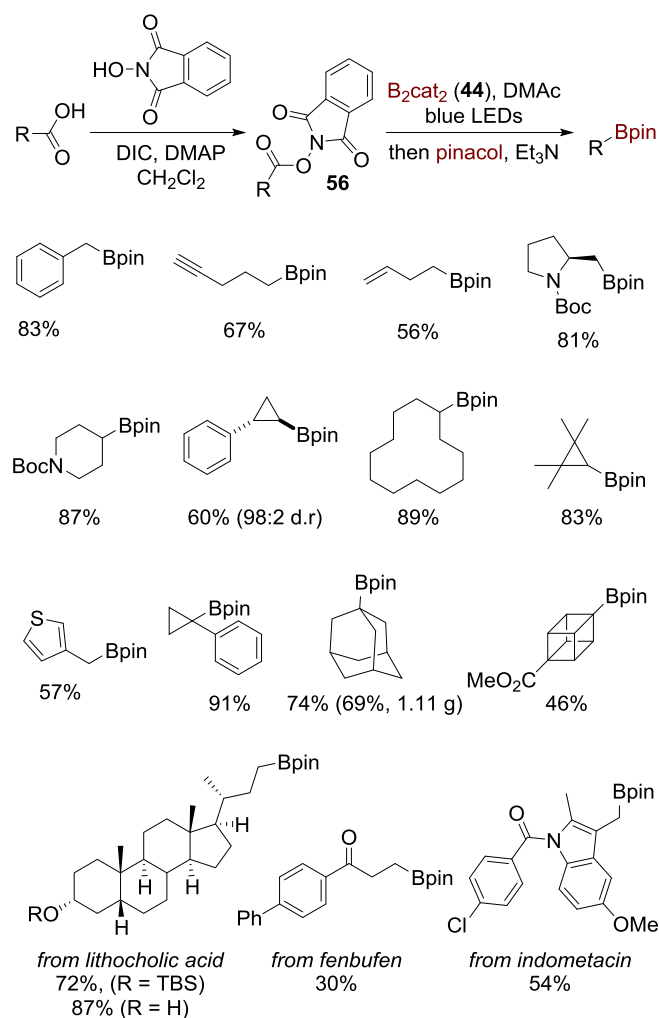


Fig. 24. Blue LED light-induced borylation of NHPI esters of alkyl carboxylic acids **56** with  $B_2cat_2$  (**44**).

In 2017, Aggarwal and coworkers reported a blue LED light-induced borylation of NHPI esters of alkyl carboxylic acids **56** with bis(catecholato)diboron (**44**) in dimethylacetamide as a solvent and in the absence of photoredox catalysts (Fig. 24) [48]. The intermediate catechol boronic esters product were converted to pinacol boronic esters by treating the reaction mixture with pinacol and triethylamine. The scope of the decarboxylative borylation encompasses NHPI esters of primary, secondary and tertiary carboxylic acids with benzylic, heterocyclic and carbocyclic substituents. The reaction tolerates a variety of functional groups, including alkenyl, alkynyl, bromo, keto and unprotected hydroxyl groups. The decarboxylative borylation was also successfully accomplished with a variety of derivatives of natural product and active pharmaceutical ingredients.

Experimental data suggest that the transformation involves a radical chain process that is more efficiently initiated photochemically than under thermal conditions (Fig. 25). In the photochemical process, a reaction of *N*-hydroxyphthalimide ester **56**, DMAc (*N,N*-dimethylacetamide) and  $B_2cat_2$  (**44**) leads to the formation of transient complex **59** that, upon photoexcitation, undergoes the B–B bond cleavage, producing DMAc-stabilized boryl radical **60** and NHPI ester-derived radical **61**. The N–O bond cleavage and decarboxylation of radical **61** produces alkyl radical **45** that is borylated with DMAc-ligated  $B_2cat_2$  complex **62**, generating boronic ester **48** and radical intermediate **60**. As with intermediate **49/49'** in Studer's borylation mechanism, intermediate **60** further serves as a radical chain carrier, producing NHPI ester-derived radical **61**. Under the thermal conditions, the reaction is initiated by formation of

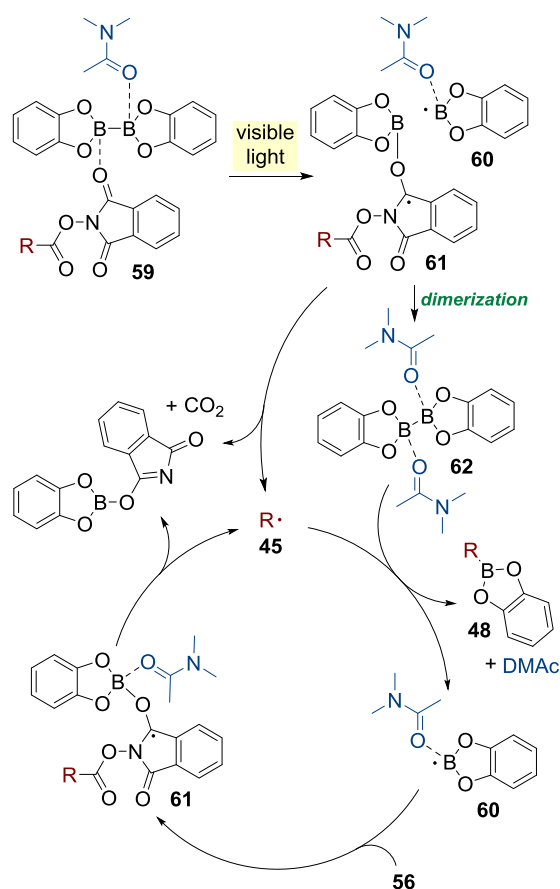


Fig. 25. Proposed mechanism for blue LED light-induced borylation of NHPI esters of alkyl carboxylic acids **56** with  $B_2cat_2$  (**44**).

DMAC-stabilized boryl radical **60** by thermal homolysis of DMAC-ligated  $B_2cat_2$  complex **62**.

#### 4. C–N borylation

Arenediazonium salts have served for a long time as a well-established source of aryl radicals [49]. In 2012, Yan and co-workers developed a visible light-induced borylation of arenediazonium salts catalyzed by the inexpensive organic dye eosin Y (Fig. 26) [50]. The reaction is compatible with substrates bearing electron-donating and electron-withdrawing groups. Somewhat lower yields were observed for *ortho*-substituted substrates. In addition, since excess diazonium salt is used, the method may be less advantageous with more valuable aniline precursors of diazonium salts.

A plausible mechanism for the borylation of arenediazonium salts is shown in Fig. 27. Visible light irradiation generates the excited state of eosin Y. Subsequent single electron transfer to arenediazonium cation **63** produces aryl radical **5**. Radical **5** then reacts with  $sp^2$ – $sp^3$  diboron adduct **64** that is formed from  $B_2pin_2$  and tetrafluoroborate anion to give radical anion **65** that is oxidized by the eosin Y-derived radical cation, thus regenerating the photocatalyst.

In 2017, Glorius and coworkers reported a visible light-induced photoredox-catalyzed conversion of *N*-acylbenzotriazoles **66** to aromatic boronic esters, sulfides, and alkylarenes bearing *ortho*-*N*-acylamino group (Fig. 28) [51]. Mechanistically, upon illumination, photocatalyst  $Ir^{III}$  is promoted to excited state  $^*Ir^{III}$  that donates one electron to benzotriazole **66** providing reactive intermediate **67** and the oxidizing  $Ir^{IV}$  species (Fig. 29). A single electron transfer takes place between the  $Ir^{IV}$  species and reductive quencher amine **68**, forming a radical cation **69** and regenerating the  $Ir^{III}$  photocatalyst. Radical anionic intermediate **67** then undergoes nitrogen extrusion to give radical **70** that subsequently engages  $B_2pin_2$  in the homolytic borylation process. The large measured quantum yield for the borylation ( $\Phi = 64.7$ ) indicates that a radical chain reaction pathway is operative.

The borylation tolerated both electron-donating and electron-withdrawing groups in the benzotriazole core, and electron-donating groups in the benzoyl fragments (Fig. 30). However, introduction of the electron-deficient *p*-CF<sub>3</sub> substituent in the benzoyl group led to a lower yield. An additive-based robustness screen [46] was conducted to prove high functional-group tolerance of this borylation and its usefulness for the synthesis of *ortho*-

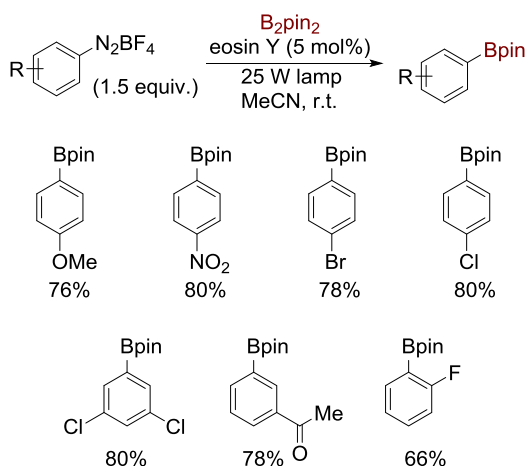


Fig. 26. Visible light-induced, eosin Y-catalyzed borylation of arenediazonium salts.

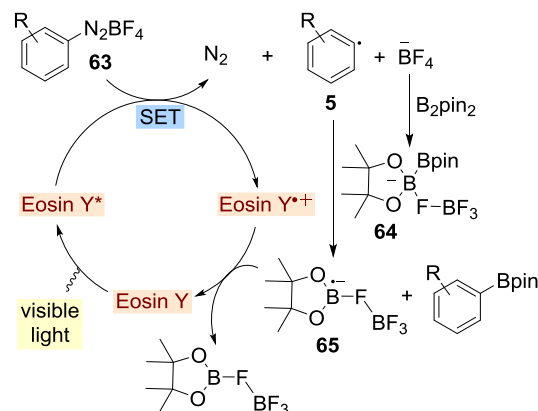


Fig. 27. Mechanism of eosin Y-photocatalyzed borylation of arenediazonium salts.

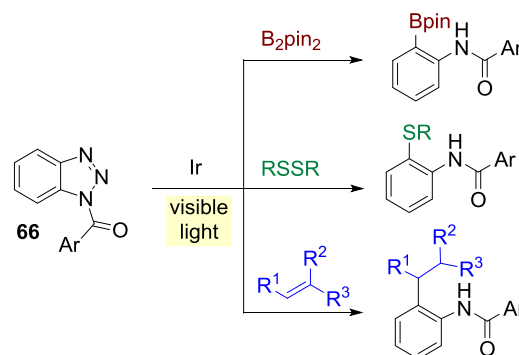


Fig. 28. General approach to borylation, thiolation and alkylation of *N*-acylbenzotriazoles.

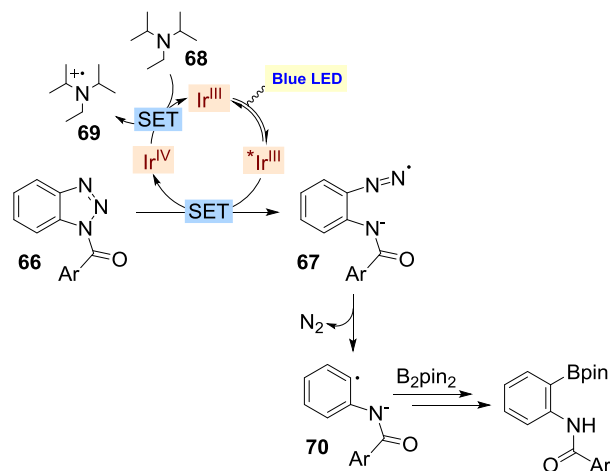
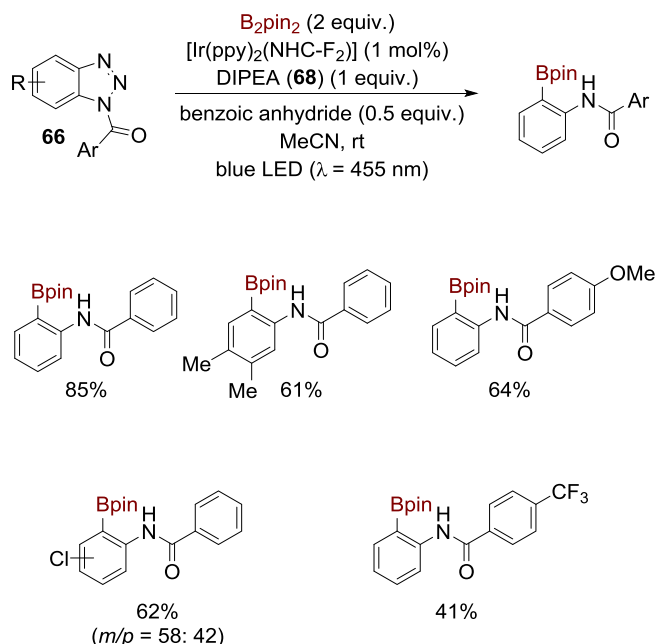
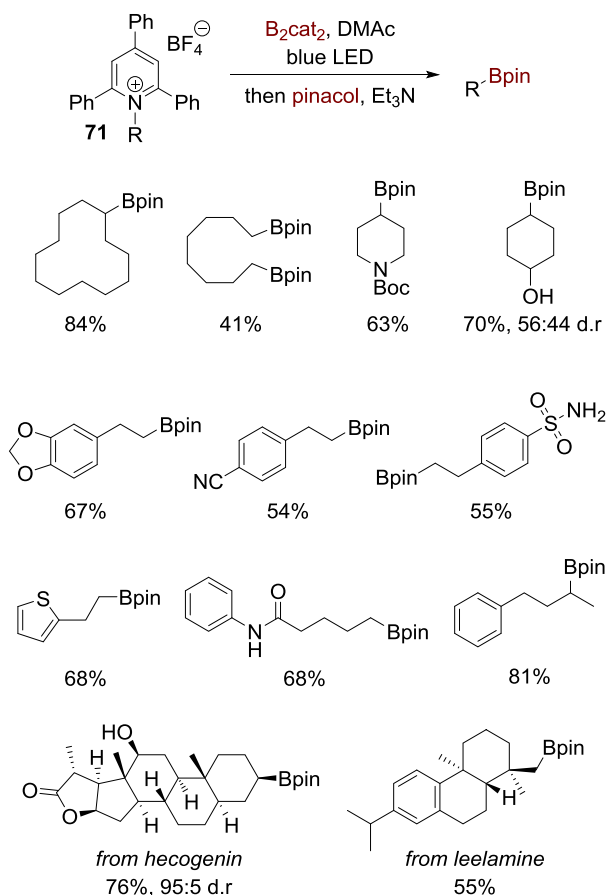


Fig. 29. Mechanism of photoredox-catalyzed borylation of *N*-acylbenzotriazoles **66**.

borylated aniline derivatives. Indeed, the borylation reaction performed well in the presence of nitriles, aryl halides, alkenes, alkynes, esters, amides, furans, thiophenes, pyridines, and *N*-protected pyrroles. On the other hand, alcohols, alkyl chlorides and alkyl amines did not inhibit the formation of products but were partially consumed under the reaction conditions. While 2-chloroquinoline, *N*-methylimidazole, and indole slightly lowered the yield, they remained intact. In contrast, aniline completely shut

Fig. 30. Representative products of borylation of *N*-acylbenzotriazoles **66**.

down the reaction and was to a substantial extent consumed. By changing photocatalyst and solvents, Glorius and coworkers were

Fig. 31. Blue LED light-induced borylation of *N*-alkylpyridinium salts **71** with  $B_2cat_2$  (**44**).

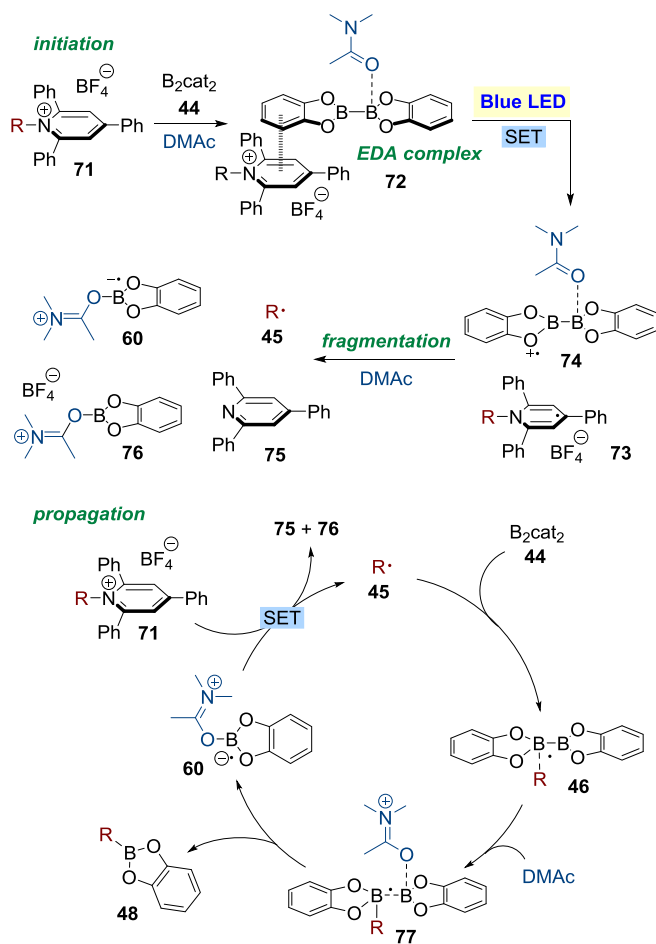
also able to extend the method to synthesis of *o*-alkyl- and *o*-alkylthio-*N*-arylbenzamides in moderate to good yields.

In 2018, a photoinduced deaminative borylation, in which *N*-alkylpyridinium salts **71** were converted to alkylboronic esters, was reported by Aggarwal group (Fig. 31) [52].

The use of  $B_2cat_2$  (**44**) was essential, as no products were observed with other diboron reagents, such as  $B_2pin_2$  or  $B_2(OH)_4$ . As with other similar photoinduced borylation reactions discussed in this review, use of an amide solvent, DMAc in this case, was crucial for achieving high yields.

Salts **71** derived from a variety of secondary amines, including those bearing free alcohols and protected amines were successfully converted to Bpin esters in good yields, after treatment of boronic esters **48** with pinacol and triethylamine. Primary alkylboronic esters were also produced in good to excellent yields from the corresponding primary alkylamines. Many functional groups, e.g., carboxylic acids, esters, ethers, amides, alkynes, alkenes and with aromatic heterocycles were tolerated. Natural product-derived substrates, e.g., leelamine and lysine gave corresponding boronic esters in good yields. Steroids hecogenin and tigogenin proved compatible with this transformation, giving corresponding borylation products with good yields and high diastereoselectivity. Amines bearing tertiary alkyl groups did not form the pyridinium salts **71**, thus no tertiary alkylboronic esters were prepared.

It is hypothesized that in the initiation phase, electron donor–acceptor (EDA) complex **72** between *N*-alkylpyridinium salt

Fig. 32. Mechanism of blue LED light-induced borylation of *N*-alkylpyridinium salts **71** with  $B_2cat_2$  (**44**).

**71**, B<sub>2</sub>cat<sub>2</sub>·(**44**), and DMAc is formed (Fig. 32). A photoinduced SET process within complex **72** triggers a radical chain process, generating *N*-alkylpyridinium-derived radical **73** and DMAc-stabilized B<sub>2</sub>cat<sub>2</sub>-derived radical **74**. Radical **73** further fragments to give alkyl radical **45** and 2,4,6-triphenylpyridine (**75**). On the other hand, radical **74** reacts with DMAc to give boryl-derived radical **60** and boryl product **76**. The chain propagation then proceeds with the reaction between alkyl radical **45** and B<sub>2</sub>cat<sub>2</sub> to give radical intermediate **46** that subsequently forms adduct **77** with DMAc. The fragmentation of adduct **77** affords alkylboronic ester **48** and regenerates boryl radical **60**. Radical **60** further reacts with *N*-alkylpyridinium salt **71**, propagating the radical chain. The mechanism was supported by experimental studies that confirm formation of an EDA complex and a high photochemical quantum yield ( $\Phi = 7$ ).

## 5. Other photoinduced reactions of organoboron compounds

In 2015, Ogawa and coworkers developed a metal-free photoinduced diborylation of terminal alkynes (Fig. 33) [53]. The transformation was applied to different alkynes to prepare different diborylated alkenes with the variation of *E/Z* ratio from 24:76 to 34:66. The reaction performed well with terminal alkynes bearing ester, chloro, cyano and phenyl groups. Phenylacetylene failed to form the product due to the competing polymerization occurring under the reaction conditions.

Mechanistic investigation indicated that the reaction proceeded through a radical pathway (Fig. 34). Indeed, the use of radical initiator 2,2'-azobis(isobutyronitrile) (AIBN) promoted diboration in the dark, albeit sluggishly, with 7% yield. An EPR study confirmed the presence of radical species in the reaction mixture with  $g = 2.0035$ , which was proposed to be a boryl-centered radical, since the  $g$  value did not correspond to a sulfide-centered radical [54]. It was suggested that the sulfide facilitates the cleavage of the B–B bond, giving rise to boryl radical **78**, which may result from the coordination of sulfur to boron atom or energy transfer. Boryl radical **78** combines with the alkyne in a chain process yielding product and regenerating the disulfide catalyst.

One year later, Owaga and coworkers reported an improved alkyne diboration method that gave a higher *trans*-selectivity with phosphines as photocatalysts (Fig. 35) [55]. Addition of B<sub>2</sub>pin<sub>2</sub> to alkynes proceeded well in the presence of relatively bulky phosphines, electron donating substituted aryl phosphines or diarylalkylphosphines. However, the reaction was completely shut

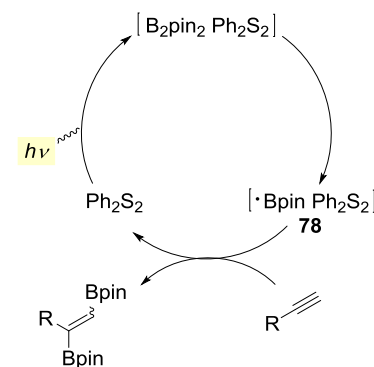


Fig. 34. Plausible mechanism of disulfide-catalyzed diboration of alkynes.

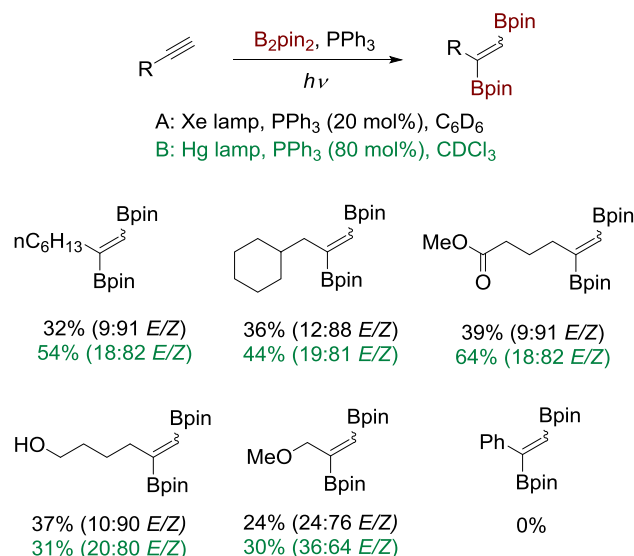


Fig. 35. Photoinduced phosphine-catalyzed diboration of alkynes.

down, when electron-deficient phosphines, trialkylphosphines and phosphine oxides were employed. Two reaction conditions were used for diborylation reactions (Fig. 35). While the use of xenon lamp with catalytic quantities of PPh<sub>3</sub> (condition A) gave higher *trans*-selectivity, the use of high-pressure Hg lamp with near-stoichiometric quantities of PPh<sub>3</sub> (condition B) gave higher yields.

Aliphatic alkynes bearing cyano, chloro, ester, ether and hydroxy groups were successfully converted to diborylated alkenes in moderate yields. As with the diphenyl disulfide-catalyzed diborylation reaction, phenylacetylene was a challenging substrate due to polymerization. The similar EPR  $g$  value as in their first report [53] and the lack of pronounced solvent effects on the product yield indicate that the reaction proceeds by a boryl radical pathway.

As shown in Fig. 36, it was suggested that PPh<sub>3</sub> coordinates to B<sub>2</sub>pin<sub>2</sub> affording intermediate **79** that undergoes homolytic cleavage to generate radicals **80** and **81**. Between these two species, **80** is more reactive, and it attacks the alkyne substrate to form vinyl radical **82**. The ensuing homolytic substitution reaction between vinyl radical **82** and B<sub>2</sub>pin<sub>2</sub> produces diboration product **83** and regenerates boryl radical **80** that proceeds to combine with radical **81**, giving rise to adduct **79**. The *trans*-selectivity was explained by the steric interactions between B<sub>2</sub>pin<sub>2</sub> and vinyl radical **82**, as well as the photoisomerization mediated by PPh<sub>3</sub>.

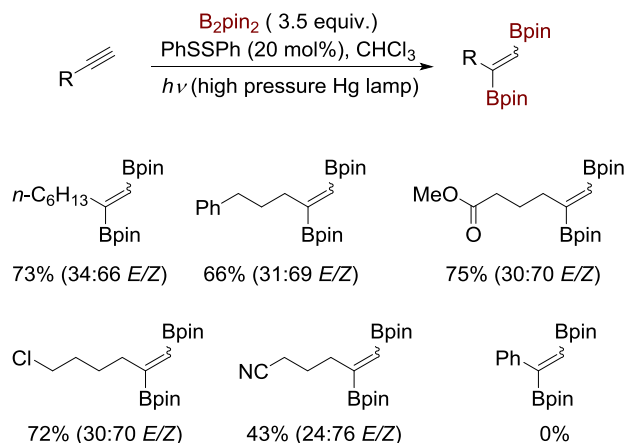


Fig. 33. Photoinduced, disulfide-catalyzed diboration of alkynes.



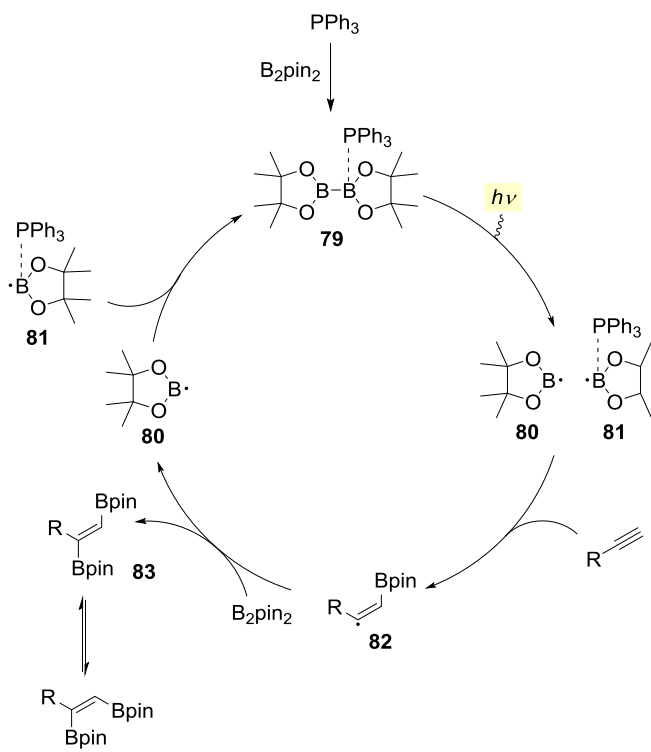


Fig. 36. Plausible mechanism of photoinduced phosphine-catalyzed diboration of alkynes.

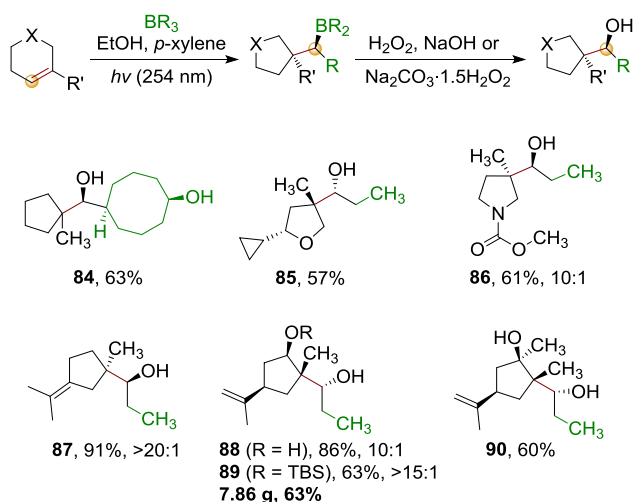


Fig. 37. Photoinduced carboborative ring contraction.

In 2017, Larionov and coworkers developed a method for conversion of readily accessible unsaturated six-membered ring precursors to less abundant five-membered carbocycles and heterocycles using photochemical activation that they termed carboborative ring contraction (Fig. 37) [56]. Optimization experiments showed that the reaction proceeded faster and with higher yields in more polar solvents, for example ethanol, dioxane or THF and in the presence of *p*-xylene as a photosensitizer under UV irradiation (254 nm).

A variety of trialkylboranes were readily prepared and reacted

with unsaturated six-membered carbocycles and heterocycles to obtain desired products in moderate to good yields. Remarkably, 9-methoxy-9-borabicyclo[3.3.1]-nonane (9-BBN-OMe) was also a suitable reagent, giving the diol **84** in 63% yield after oxidation, whereas tetrahydrofuran **85** was isolated as a single diastereomer, the diastereomeric ratio was 10:1 for pyrrolidine **86**. Terpenoids and their derivatives including terpinolene (**87**), (*R,R*)-carveol (**88**, **89**) and its tertiary alcohol derivative **90** afforded corresponding products in good yields and high stereoselectivity, also on gram scales. Likewise, a number of B-ring norsteroids were also prepared in good yields and with high regio- and stereoselectivity (Fig. 38) from cholesterol, diosgenin, pregnenolone derivatives, dehydroepiandrosterone and azasteroids with various trialkylboranes (**91–96**).

Photoinduced carboborative ring contraction also enabled a concise total synthesis of artalbic acid (**97**) that commenced with the photoinduced carboborative ring contraction of (*S,S*)-carveol-derived TBS ether **98** with triethylborane, followed by a sequence of oxidations with trimethylamine *N*-oxide and Dess–Martin periodinane to give ketone **99** (Fig. 39). Subsequent desaturation of the side chain via  $\alpha$ -selenylation and hydrogen peroxide-induced selenoxide elimination afforded vinyl ketone **100** that was subjected to the phosphine-catalyzed Rauhut–Currier reaction with acrylonitrile to give nitrile **101**. Given the sensitive nature of nitrile **101**, the synthesis was completed by hydrolysis of nitrile **101** using two mild protocols. In the first protocol, desilylation of nitrile **101** afforded alcohol **102** that was hydrolyzed biocatalytically with nitrilase at pH 7.2. In the second protocol, hydration of nitrile **101** using Parkins catalyst **103** produced primary amide **104** that was then activated by double *N*-carbamidation with Boc<sub>2</sub>O, and basic hydrolysis at room temperature.

The reaction is thought to proceed by photosensitized isomerization to strained and highly reactive *E*-isomer of cyclohexene **105**, followed by addition of organoborane to the equatorial position on C2 to give zwitterionic intermediate **106**. Subsequent 1,2-migration of the C3 atom to C1, accompanied by a shift of one alkyl group R from boron to C2 position produces cyclopentanes with two new stereocenters (Fig. 40) either by inversion or retention pathway. The migration of the alkyl group, according to experimental data, favors the inversion pathway, forming the major product **107** rather than the retention pathway, which results in the minor product **108**.

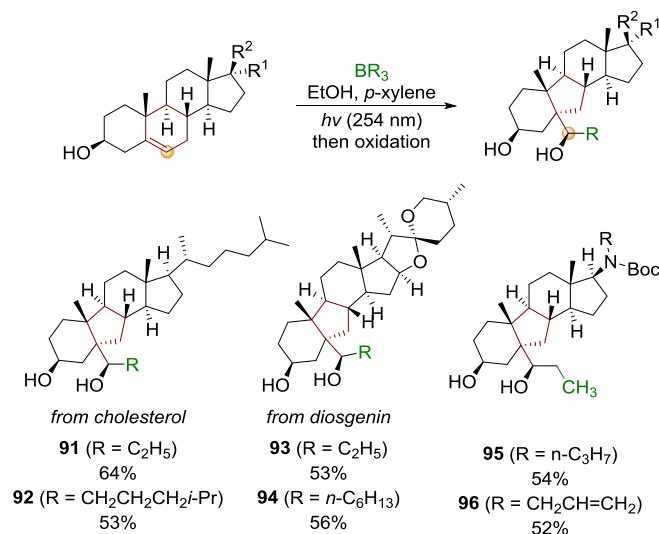


Fig. 38. Photoinduced carboborative ring contraction of steroid substrates.



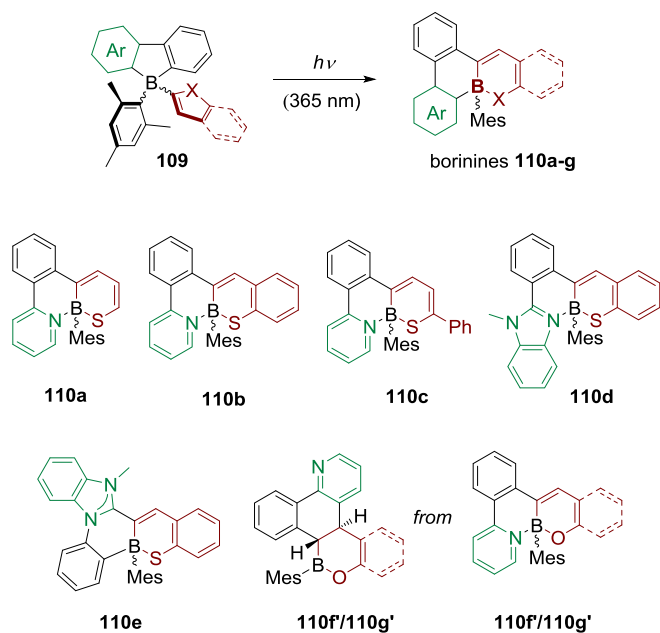


Fig. 41. Photoinduced isomerization of organoboron compounds **109** to borinines **110**.

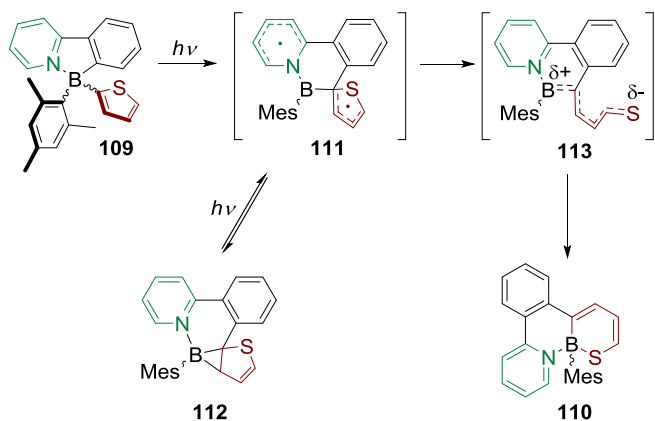


Fig. 42. Plausible mechanism of photoinduced isomerization of organoboron compounds **109** to borinines **110**.

dimethylacetamide as solvents.

The reaction has a broad scope with respect to various structurally diverse carboxylic acids. Boc-protected  $\alpha$ -amino acids that do not have a hydrogen on the  $\alpha$ -nitrogen atom reacted well, when catalyst **57** was used (e.g., products **115–117**). A stronger reducing photocatalyst **114** was required for  $\alpha$ -amino acids with a hydrogen on the  $\alpha$ -nitrogen atom and for all other carboxylic acids (e.g., products **118–122**). Substituted vinylboronic esters were also suitable substrates (e.g., products **116** and **117**). In addition, several boronate products derived from natural products (e.g., boronates **121**, **122** and active pharmaceutical ingredients (e.g., products **119**, **120**) were readily prepared using the developed protocol.

The authors propose that the reactive carboxylate anion **123** is first formed from the carboxylic acid in the reaction with cesium carbonate (Fig. 44). Subsequent one-electron oxidation with the photoexcited  $^*\text{Ir}^{\text{III}}$  catalyst leads to decarboxylation and formation

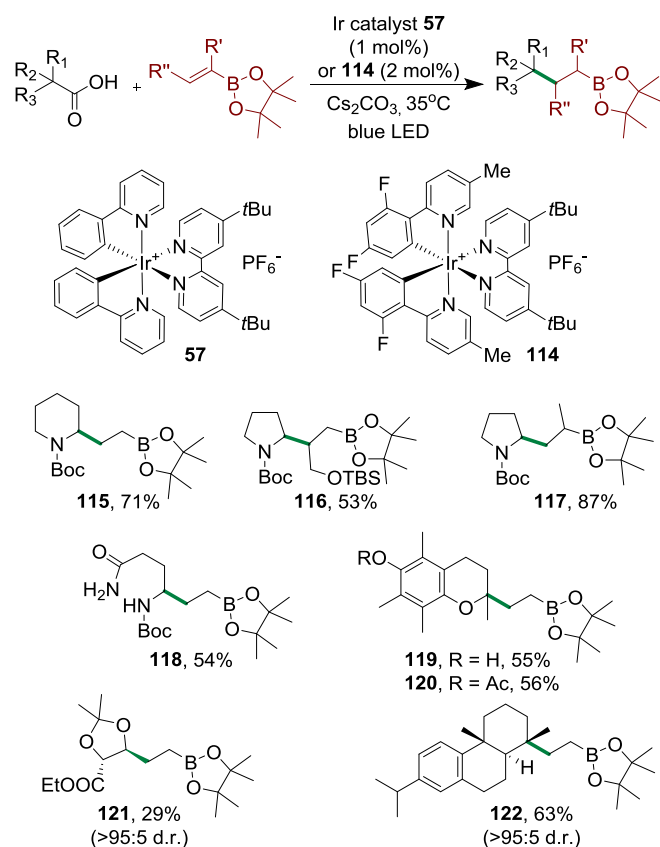


Fig. 43. Photoredox-catalyzed decarboxylative alkylation of vinylboronic esters.

of radical **124** that adds to the vinylboronic **125** ester to give  $\alpha$ -boryl alkyl radical **126** that is stabilized through  $\pi$ -donation to the boryl group. Radical **126** further undergoes reduction with the reduced  $\text{Ir}^{\text{II}}$  catalyst species to give anion **127** that is further protonated. The thermodynamic feasibility of the reduction of radical **126** by the  $\text{Ir}^{\text{II}}$  catalyst was confirmed by DFT calculations. In addition, partial deuteration was observed in the  $\alpha$ -position of the alkylboronate moiety, supporting involvement of anion **127**.

Vicinal difunctionalization is one of the most powerful and valuable transformations in organic synthesis. The 1,2-difunctionalization of alkenes that can construct two distinct chemical bonds in a single operation is an efficient tool for increasing molecular complexity. In recent years, transition metal-catalyzed carboboration has attracted significant attention. However, only few reports on transition metal-free 1,2-carboboration of alkenes have been reported [59]. In 2018, Studer and coworkers disclosed a photoinduced transition metal-free 1,2-carboboration of unactivated alkenes with  $\text{B}_2\text{cat}_2$  (**44**) as the boron source combined with perfluoroalkyl iodides as the alkyl component (Fig. 45) [43].

The reaction is particularly suitable for carboboration of monosubstituted alkenes (**128–131**), although reactive disubstituted alkenes can also be used (**132** and **133**). In the case of a 1,5-diene substrate, the carboboration occurred regioselectivity at the terminal double bond (**131**). Although perfluorobutyl iodide was used for most examples, other perfluoroalkyl iodides and sources of stabilized electrophilic radicals were used as well (**134** and **135**). The reaction is initiated by a perfluoroalkyl radical that is



Voelcker Fund, and the Brown Foundation is gratefully acknowledged.

## References

- [1] (a) T.D. James, S. Shinkai, *Top. Curr. Chem.* 218 (2002) 159; (b) R. Jelinek, S. Kolusheva, *Chem. Rev.* 104 (2004) 5987; (c) A. Pal, M. Berube, D.G. Hall, *Angew. Chem. Int. Ed.* 49 (2010) 1492; (d) J.S. Hansen, J.B. Christensen, J.F. Petersen, T. Hoeg-Jensen, J.C. Norrild, *Sens. Actuators, B* 161 (2012) 45.
- [2] (a) C.R. Wade, A.E.J. Broomsgrove, S. Aldridge, F.P. Gabbaï, *Chem. Rev.* 110 (2010) 3958; (b) X. Wu, Z. Li, X.-X. Chen, J.S. Fossey, T.D. James, Y.B. Jiang, *Chem. Soc. Rev.* 42 (2013) 8032; (c) Y. Guan, Y. Zhang, *Chem. Soc. Rev.* 42 (2013) 8106; (d) L. You, D. Zha, E.V. Anslyn, *Chem. Rev.* 115 (2015) 7840; (e) J. Wu, B. Kwon, W. Liu, E.V. Anslyn, P. Wang, J.S. Kim, *Chem. Rev.* 115 (2015) 7893.
- [3] (a) A. Suzuki, H.C. Brown, *Organic Syntheses via Boranes*, vol. 3, Aldrich Chemical Company, Milwaukee, 2003; (b) D.G. Hall (Ed.), *Boronic Acids*, second ed., Wiley-VCH, Weinheim, 2011; (c) W.R. Gutekunst, P.S. Baran, *Chem. Soc. Rev.* 40 (2011) 1976.
- [4] (a) J.B. Chen, A. Whiting, *Synthesis* 50 (2018) 3843; (b) B.S.L. Collins, C.M. Wilson, E.L. Myers, V.K. Aggarwal, *Angew. Chem. Int. Ed.* 56 (2017) 11700; (c) C.M. Crudden, D. Edwards, *Eur. J. Org. Chem.* 24 (2003) 4695.
- [5] (a) K. Kubota, E. Yamamoto, H. Ito, *J. Am. Chem. Soc.* 135 (2013) 2635; (b) K. Semba, Y. Nakao, *J. Am. Chem. Soc.* 136 (2014) 7567; (c) L. Jiang, P. Cao, M. Wang, B. Chen, B. Wang, J. Liao, *Angew. Chem. Int. Ed. Engl.* 55 (2016) 13854; (d) K.M. Logan, M.K. Brown, *Angew. Chem. Int. Ed. Engl.* 56 (2017) 851; (e) K.B. Smith, M.K. Brown, *J. Am. Chem. Soc.* 139 (2017) 7721; (f) L.J. Cheng, N. Mankad, *Angew. Chem. Int. Ed.* 57 (2018) 10328; (g) J. Lee, S. Radomkit, S. Torker, J. Del Pozo, A.H. Hoveyda, *Nat. Chem.* 10 (2018) 99; (h) K.M. Logan, S.R. Sardini, S.D. White, M.K. Brown, *J. Am. Chem. Soc.* 140 (2018) 159; (i) K.B. Smith, Y. Huang, M.K. Brown, *Angew. Chem. Int. Ed. Engl.* 57 (2018) 6146.
- [6] E.J. Corey, *Angew. Chem. Int. Ed.* 41 (2002) 1650.
- [7] (a) E. Dimitrijević, M.S. Taylor, *ACS Catal.* 3 (2013) 945; (b) K. Ishihara, *Top. Organomet. Chem.* 49 (2015) 243; (c) M.S. Taylor, *Acc. Chem. Res.* 48 (2015) 295.
- [8] (a) A. Lorbach, A. Huebner, M. Wagner, *Dalton Trans.* 41 (2012) 6048; (b) J. Liu, J.J. Lavigne, in: D.G. Hall (Ed.), *Boronic Acids*, second ed., Wiley-VCH, Weinheim, 2011; (c) F. Jäkle, *Top. Organomet. Chem.* 49 (2015) 297; (d) H.A. Yemam, A. Mahl, U. Koldemir, T. Remedès, S. Parkin, U. Greife, A. Sellinger, *Sci. Rep.* 5 (2015) 13401; (e) Y. Shoji, Y. Ikabata, Q. Wang, D. Nemoto, A. Sakamoto, N. Tanaka, J. Seino, H. Nakai, T. Fukushima, *J. Am. Chem. Soc.* 139 (2017) 2728.
- [9] (a) B.C. Das, P. Thapa, R. Karki, C. Schinke, S. Das, S. Kambhampati, S.K. Banerjee, P. Van Veldhuizen, A. Verma, L.M. Weiss, *Future Med. Chem.* 5 (2013) 653; (b) R.I. Scorei, R. Popa, *Anti Cancer Agents Med. Chem.* 10 (2010) 346; (c) T.C. Kouroukis, F.G. Baldassarre, A.E. Haynes, K. Imrie, D.E. Reece, M.C. Cheung, *Curr. Oncol.* 21 (2014) e573.
- [10] (a) E. Khotinsky, M. Melamed, *Ber. Dtsch. Chem. Ges.* 42 (1909) 3090; (b) R.L. Letsinger, I.H. Skoog, *J. Org. Chem.* 18 (1953) 895.
- [11] (a) T. Ishiyama, M. Murata, N. Miyauro, *J. Org. Chem.* 60 (1995) 7508; (b) M. Murata, S. Watanabe, Y. Masuda, *J. Org. Chem.* 62 (1997) 6458; (c) T. Ishiyama, N. Miyauro, *J. Organomet. Chem.* 611 (2000) 392; (d) T. Ishiyama, N. Miyauro, in: D.G. Hall (Ed.), *Boronic Acids*, second ed., Wiley-VCH, Weinheim, 2011; (e) W.K. Chow, O.Y. Yuen, P.Y. Choy, C.M. So, C.P. Lau, W.T. Wong, F.Y. Kwong, *RSC Adv.* 3 (2013) 12518.
- [12] (a) G.A. Molander, S.L.J. Trice, S.D. Dreher, *J. Am. Chem. Soc.* 132 (2010) 17701; (b) G.A. Molander, S.L.J. Trice, S.M. Kennedy, S.D. Dreher, M.T. Tudge, *J. Am. Chem. Soc.* 134 (2012) 11667; (c) G.A. Molander, S.L.J. Trice, S.M. Kennedy, *J. Org. Chem.* 77 (2012) 8678; (d) G.A. Molander, S.L. Trice, S.M. Kennedy, *Org. Lett.* 14 (2012) 4814; (e) G.A. Molander, L.N. Cavalcanti, C. Garcia-Garcia, *J. Org. Chem.* 78 (2013) 6427.
- [13] (a) J.-Y. Cho, M.K. Tse, D. Holmes, R.E. Maleczka, M.R. Smith, *Science* 295 (2002) 305; (b) I.A.I. Mkhaliid, J.H. Barnard, T.B. Marder, J.M. Murphy, J.F. Hartwig, *Chem. Rev.* 110 (2010) 890; (c) J.F. Hartwig, *Acc. Chem. Res.* 45 (2012) 864; (d) T. Stahl, K. Muether, Y. Ohki, K. Tatsumi, M. Oestreich, *J. Am. Chem. Soc.* 135 (2013) 10978; (e) D.E. Stephens, O.V. Larionov, *Tetrahedron* 71 (2015) 8683.
- [14] (a) E. Yamamoto, K. Izumi, Y. Horita, H. Ito, *J. Am. Chem. Soc.* 134 (2012) 19997; (b) Y. Nagashima, R. Takita, K. Yoshida, K. Hirano, M. Uchiyama, *J. Am. Chem. Soc.* 135 (2013) 18730; (c) J. Zhang, H.-H. Wu, J. Zhang, *Eur. J. Org. Chem.* 28 (2013) 6263; (d) E. Yamamoto, K. Izumi, Y. Horita, S. Ukigai, H. Ito, *Top. Catal.* 57 (2014) 940; (e) S.K. Bose, T.B. Marder, *Org. Lett.* 16 (2014) 4562; (f) E. Yamamoto, S. Ukigai, H. Ito, *Chem. Sci.* 6 (2015) 2943; (g) R. Uematsu, E. Yamamoto, S. Maeda, H. Ito, T. Taketsugu, *J. Am. Chem. Soc.* 137 (2015) 4090; (h) S.K. Bose, A. Deissenberger, A. Eichhorn, P.G. Steel, Z. Lin, T.B. Marder, *Angew. Chem. Int. Ed.* 54 (2015) 11843; (i) L. Zhang, L. Jiao, *J. Am. Chem. Soc.* 139 (2017) 607.
- [15] (a) T.S. De Vries, A. Prokofjevs, E. Vedejs, *Chem. Rev.* 112 (2012) 4246; (b) M.J. Ingleson, *Synlett* 23 (2012) 1411; (c) M.J. Ingleson, *Top. Organomet. Chem.* 49 (2015) 39; (d) A.J. Warner, J.R. Lawson, V. Fasano, M.J. Ingleson, *Angew. Chem. Int. Ed.* 54 (2015) 11245; (e) S. Tanaka, Y. Saito, T. Yamamoto, T. Hattori, *Org. Lett.* 20 (2018) 1828; (f) A. Issaian, K.N. Tu, S.A. Blum, *Acc. Chem. Res.* 50 (2017) 2598.
- [16] (a) F. Mo, Y. Jiang, D. Qiu, Y. Zhang, J. Wang, *Angew. Chem. Int. Ed.* 49 (2010) 1846; (b) J. Yu, L. Zhang, G. Yan, *Adv. Synth. Catal.* 354 (2012) 2625; (c) C. Zhu, M. Yamane, *Org. Lett.* 14 (2012) 4560; (d) D. Qiu, L. Jin, Z. Zheng, H. Meng, F. Mo, X. Wang, Y. Zhang, J. Wang, *J. Org. Chem.* 78 (2013) 1923; (e) D. Qiu, Y. Zhang, J. Wang, *Org. Chem. Front.* 1 (2014) 422; (f) W. Erb, A. Hellal, M. Albini, J. Rouden, J. Blanchet, *Chem. Eur. J.* 20 (2014) 6608; (g) C.-J. Zhao, D. Xue, Z.H. Jia, C. Wang, J. Xiao, *Synlett* 25 (2014) 1577.
- [17] (a) C. Li, J. Wang, L.M. Barton, S. Yu, M. Tian, D.S. Peters, M. Kumar, A.W. Yu, K.A. Johnson, A.K. Chatterjee, M. Yan, P.S. Baran, *Science* 356 (2017) eam7355; (b) J. Wang, M. Shang, H. Lundberg, K.S. Feu, S.J. Hecker, T. Qin, D.G. Blackmond, P.S. Baran, *ACS Catal.* 8 (2018) 9537.
- [18] (a) L. Schutt, N.G. Bunce, in: W.M. Horspool, F. Lenci (Eds.), *CRC Handbook of Organic Photochemistry and Photobiology*, second ed., CRC Press, Boca Raton, 2004; (b) A. Albini, M. Fagnoni, *Handbook of Synthetic Photochemistry*, Wiley-VCH, Weinheim, 2010; (c) A. Albini, M. Fagnoni, *Photochemically-generated Intermediates in Synthesis*, John Wiley & Sons, Inc., Hoboken, 2013.
- [19] (a) J.F. Bunnett, *Acc. Chem. Res.* 11 (1978) 413; (b) C. Kapire, I. Siddik, in: W.M. Horspool, F. Lenci (Eds.), *CRC Handbook of Organic Photochemistry and Photobiology*, second ed., CRC Press, Boca Raton, 2004; (c) C. Uyeda, Y.C. Tan, G.C. Fu, J.C. Peters, *J. Am. Chem. Soc.* 135 (2013) 9548; (d) Y.C. Tan, J.M. Munoz-Molina, G.C. Fu, J.C. Peters, *Chem. Sci.* 5 (2014) 2831; (e) L. Li, W. Liu, H. Zeng, X. Mu, G. Cosa, Z. Mi, C.-J. Li, *J. Am. Chem. Soc.* 137 (2015) 8328.
- [20] (a) V. Dichiarante, M. Fagnoni, A. Albini, *Angew. Chem. Int. Ed.* 46 (2007) 6495; (b) M.E. Buden, J.F. Guastavino, R.A. Rossi, *Org. Lett.* 15 (2013) 1174; (c) J. Ruch, A. Aubin, G. Erbland, A. Fortunato, J.-P. Goddard, *Chem. Comm.* 52 (2016) 2326.
- [21] (a) M. Mella, P. Coppo, B. Guizzardi, M. Fagnoni, M. Freccero, A. Albini, *J. Org. Chem.* 66 (2001) 6344; (b) B. Guizzardi, M. Mella, M. Fagnoni, A. Albini, *Chem. Eur. J.* 9 (2003) 1549; (c) X.L. Zheng, L. Yang, W.Y. Du, A.S. Ding, H. Guo, *Chem. Asian J.* 9 (2014) 439.
- [22] (a) J. Grimshaw, A.P. de Silva, *Chem. Soc. Rev.* 10 (1981) 181; (b) Y.T. Park, N.W. Song, C.G. Hwang, K.W. Kim, D. Kim, *J. Am. Chem. Soc.* 119 (1997) 10677; (c) S.C. Lu, X.X. Zhang, Z.J. Shi, Y.W. Ren, B. Li, W. Zhang, *Adv. Synth. Catal.* 351 (2009) 2839.
- [23] (a) A.G. Davies, B.P. Roberts, J.C. Scaiano, *J. Chem. Soc. B* (1971) 2171; (b) K. Nozaki, K. Oshima, K. Utimoto, *Bull. Chem. Soc. Jpn.* 64 (1991) 403; (c) H.C. Brown, M.M. Midland, *Angew. Chem., Int. Ed. Engl.* 11 (1972) 692; (d) C. Ollivier, P. Renaud, *Chem. Rev.* 101 (2001) 3415.
- [24] (a) D. Lu, C. Wu, P. Li, *Chem. Eur. J.* 20 (2014) 1630; (b) D. Lu, C. Wu, P. Li, *Org. Lett.* 16 (2014) 1486.
- [25] (a) C. Kleeborg, A.G. Crawford, A.S. Batsanov, P. Hodgkinson, D.C. Apperley, M.S. Cheung, Z. Lin, T.B. Marder, *J. Org. Chem.* 77 (2012) 785; (b) S. Pietsch, E.C. Neeve, D.C. Apperley, R. Bertermann, F. Mo, D. Qiu, M.S. Cheung, L. Dang, J. Wang, U. Radius, Z. Lin, C. Kleeborg, T.B. Marder, *Chem. Eur. J.* 21 (2015) 7082.
- [26] (a) J.E. Leffler, E. Dolan, T. Tanigaki, *J. Am. Chem. Soc.* 87 (1965) 927; (b) J. Lalevee, N. Blanchard, A.-C. Chan, M.-A. Tehfe, X. Allonas, J.-P. Fouassier, *J. Phys. Org. Chem.* 22 (2009) 986; (c) D.P. Curran, A. Solov'yev, M.M. Brahmi, L. Fensterbank, M. Malacria, E. Lacote, *Angew. Chem. Int. Ed.* 50 (2011) 10294.
- [27] A.M. Mfuh, J.D. Doyle, B. Chhetri, H.D. Arman, O.V. Larionov, *J. Am. Chem. Soc.* 138 (2016) 2985.
- [28] Y.-R. Luo, *Comprehensive Handbook of Chemical Bond Energies*, CRC Press, Boca Raton, FL, 2007.
- [29] A.M. Mfuh, B.D. Schneider, W. Cruces, O.V. Larionov, *Nat. Protoc.* 12 (2017) 604.
- [30] A.M. Mfuh, V.T. Nguyen, B. Chhetri, J.E. Burch, J.D. Doyle, V.N. Nesterov,



- H.D. Arman, O.V. Larionov, *J. Am. Chem. Soc.* 138 (2016) 8408.
- [31] K. Chen, S. Zhang, P. He, P. Li, *Chem. Sci.* 7 (2016) 3676.
- [32] K. Chen, M.S. Cheng, Z. Lin, P. Li, *Org. Chem. Front.* 3 (2016) 875.
- [33] K. Mukai, D.P. de Sant'Ana, Y. Hirooka, E.V. Mercado-Marin, D.E. Stephens, K.G. Kou, S.C. Richter, N. Kelley, R. Sarpong, *Nat. Chem.* 10 (2018) 38.
- [34] H. Yang, H. Fu, *Org. Lett.* 18 (2016) 5248.
- [35] C.K. Prier, D.A. Rankic, D.W. MacMillan, *Chem. Rev.* 113 (2013) 5322.
- [36] D.D.M. Wayner, J.J. Dannenberg, D. Griller, *Chem. Phys. Lett.* 131 (1986) 189.
- [37] J. Nguyen, E. D'Amato, J. Narayanam, C. Stephenson, *Nat. Chem.* 4 (2012) 854.
- [38] (a) G. Radivoy, F. Alonso, M. Yus, *Tetrahedron* 55 (1999) 14479;  
(b) A. Jutand, S. Negri, A. Mosleh, *J. Chem. Soc., Chem. Commun.* (1992) 1729.
- [39] (a) L. Li, W. Liu, X. Mu, Z. Mi, C.-J. Li, *Nat. Protoc.* 11 (2016) 1948;  
(b) L. Li, W. Liu, H. Zeng, X. Mu, G. Cosa, Z. Mi, C.-J. Li, *J. Am. Chem. Soc.* 137 (2015) 8328.
- [40] W. Liu, X. Yang, Y. Gao, C.-J. Li, *J. Am. Chem. Soc.* 139 (2017) 8621.
- [41] (a) K. Suzuki, F. Tang, Y. Kikukawa, K. Yamaguchi, N. Mizuno, *Angew. Chem. Int. Ed.* 53 (2014) 5356;  
(b) H. Yin, P.J. Carroll, J.M. Anna, E.J. Schelter, *J. Am. Chem. Soc.* 137 (2015) 9234;  
(c) H. Yin, P.J. Carroll, B.C. Manor, J.M. Anna, E.J. Schelter, *J. Am. Chem. Soc.* 138 (2016) 5984;  
(d) H. Yin, Y. Jin, J.E. Hertzog, K.C. Mullane, P.J. Carroll, B.C. Manor, J.M. Anna, E.J. Schelter, *J. Am. Chem. Soc.* 138 (2016) 16266.
- [42] Y. Qiao, Q. Yang, E. Schelter, *Angew. Chem. Int. Ed.* 57 (2018) 10999.
- [43] Y. Cheng, C. Mück-Lichtenfeld, A. Studer, *J. Am. Chem. Soc.* 140 (2018) 6221. For a brief discussion, see: S. Jin, O.V. Larionov, *Chem* 4 (2018) 1184.
- [44] Y. Cheng, C. Mück-Lichtenfeld, A. Studer, *Angew. Chem. Int. Ed.* (2018), <https://doi.org/10.1002/anie.201810782>.
- [45] L. Candish, M. Teders, F. Glorius, *J. Am. Chem. Soc.* 139 (2017) 7440.
- [46] K.D. Collins, F. Glorius, *Nat. Chem.* 5 (2013) 597.
- [47] D. Hu, L. Wang, P. Li, *Org. Lett.* 19 (2017) 2770.
- [48] A. Fawcett, J. Pradeilles, Y. Wang, T. Mutsuga, E.L. Myers, V.K. Aggarwal, *Science* 357 (2017) 283.
- [49] M.R. Heinrich, *Chem. Eur. J.* 15 (2009) 820.
- [50] J. Yu, L. Zhang, G. Yan, *Adv. Synth. Catal.* 354 (2012) 2625.
- [51] M. Teders, A. Gomez-Suarez, L. Pitzer, M.N. Hopkinson, F. Glorius, *Angew. Chem. Int. Ed.* 56 (2017) 902.
- [52] J. Wu, L. He, A. Noble, V.K. Aggarwal, *J. Am. Chem. Soc.* 140 (2018) 10700.
- [53] A. Yoshimura, Y. Takamachi, L.-B. Han, A. Ogawa, *Chem. Eur. J.* 21 (2015) 13930.
- [54] H. Taniguchi, *J. Phys. Chem.* 88 (1984) 6245.
- [55] A. Yoshimura, Y. Takamachi, K. Mihara, T. Saeki, S.-I. Kawaguchi, L.-B. Han, A. Nomoto, A. Ogawa, *Tetrahedron* 72 (2016) 7832.
- [56] S. Jin, V.T. Nguyen, H.T. Dang, D.P. Nguyen, H.D. Arman, O.V. Larionov, *J. Am. Chem. Soc.* 139 (2017) 11365.
- [57] S.K. Møllerup, C. Li, J. Radtke, X. Wang, Q.S. Li, S. Wang, *Angew. Chem. Int. Ed.* 57 (2018) 9634.
- [58] A. Noble, R.S. Mega, D. Pflästerer, E.L. Myers, V.K. Aggarwal, *Angew. Chem. Int. Ed.* 57 (2018) 2155.
- [59] (a) R.L. Melen, L.C. Wilkins, B.M. Kariuki, H. Wade, L.H. Gade, A.S.K. Hashmi, D.W. Stephan, M.M. Hansmann, *Organometallics* 34 (2015) 4127;  
(b) A. Yamazaki, K. Nagao, T. Iwai, H. Ohmiya, M. Sawamura, *Angew. Chem. Int. Ed.* 57 (2018) 3196;  
(c) J.R. Sanzone, C.T. Hu, K.A. Woerpel, *J. Am. Chem. Soc.* 139 (2017) 8404.